

AMERICAN UNIVERSITY OF BEIRUT

LTE RADIO NETWORK PLANNING UNDER
UNCERTAINTY

by

URSULA CAMILLE CHALLITA

A thesis

submitted in partial fulfillment of the requirements
for the degree of Master of Engineering
to the Department of Electrical and Computer Engineering
of the Faculty of Engineering and Architecture
at the American University of Beirut

Beirut, Lebanon
February 2014

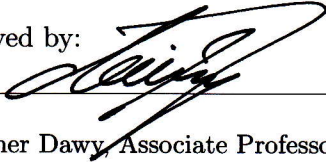
AMERICAN UNIVERSITY OF BEIRUT

LTE RADIO NETWORK PLANNING UNDER UNCERTAINTY

by

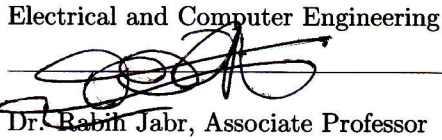
URSULA CAMILLE CHALLITA

Approved by:



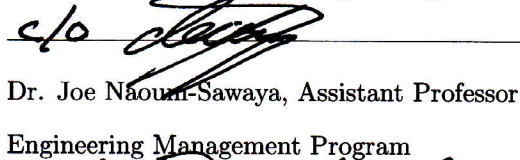
Dr. Zaher Dawy, Associate Professor
Electrical and Computer Engineering

Advisor



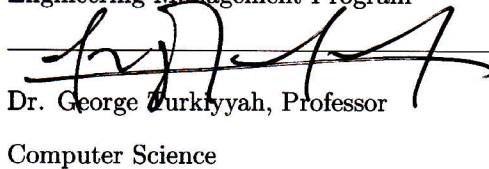
Dr. Rabin Jabr, Associate Professor
Electrical and Computer Engineering

Member of Committee



Dr. Joe Naoun-Sawaya, Assistant Professor
Engineering Management Program

Member of Committee



Dr. George Turkiyyah, Professor
Computer Science

Member of Committee

Date of thesis defense: February 5, 2014

AMERICAN UNIVERSITY OF BEIRUT

THESIS, DISSERTATION, PROJECT RELEASE FORM

Student Name: _____
 Last First Middle

Master's Thesis Master's Project Doctoral Dissertation

I authorize the American University of Beirut to: (a) reproduce hard or electronic copies of my thesis, dissertation, or project; (b) include such copies in the archives and digital repositories of the University; and (c) make freely available such copies to third parties for research or educational purposes.

I authorize the American University of Beirut, **three years after the date of submitting my thesis, dissertation, or project**, to: (a) reproduce hard or electronic copies of it; (b) include such copies in the archives and digital repositories of the University; and (c) make freely available such copies to third parties for research or educational purposes.

Signature

Date

Acknowledgements

First and foremost, I would like to thank God, the Almighty, for his blessings, and for giving me strength and patience during this research project.

I would like to thank my advisor Dr. Zaher Dawy for his guidance, assistance and constructive comments during this academic endeavor.

I am deeply grateful to Dr. George Turkiyyah for his teachings, guidance and consistent assistance for the completion of this thesis. I also express my thanks to Dr. Joe Naoum-Sawaya and Dr. Rabih Jabr for extending their support.

I would like to express my thanks and appreciation to the faculty and staff of the Electrical and Computer Engineering department.

My sincere gratitude is hereby extended to my family, friends and whoever gave me support and encouragement during my graduate studies and helped me in fulfilling this thesis work.

An Abstract of the Thesis of

Ursula Camille Challita for Master of Engineering
Major: Electrical and Computer Engineering

Title: LTE Radio Network Planning under Uncertainty

Radio network planning and optimization (RNPO) is an essential process for cellular operators and has a significant impact on the operation and cost of the resulting network. The conventional approach for planning cellular networks does not take into account the uncertainty aspects present in the network and considers a deterministic model instead. For instance, the traffic distribution of the users is usually taken at hours of peak demand and the impact of channel variation is modeled using fixed power budgets. Neglecting these uncertain parameters in the planning process leads to performance variation and, thus, requires notable efforts for post-deployment optimization. In this thesis, we adopt a stochastic optimization approach for optimizing cellular network planning under uncertainty. We propose two problem formulations for planning LTE networks taking into account the uncertainty in the location and number of users in addition to the uncertainty in the signal and interference levels. In the first part, an optimization framework is developed for planning LTE cellular networks under demand uncertainty. A two-stage deterministic equivalent of the problem is formulated and solved to optimality. Moreover, a dynamic on/off switching algorithm is developed in order to minimize the energy consumption at off-peak hours. In the second part, a chance constraint approach is adopted for solving the problem of LTE radio network planning under the uncertainty of the signal and interference levels. Site selection and site placement formulations are developed. Both problems are shown to be NP-hard and, thus, a heuristic algorithm is proposed that can achieve notable performance gains compared to conventional approaches with relatively low computational complexity. Performance results are presented and assessed for several cellular network scenarios in order to highlight the effectiveness of the proposed algorithms.

Contents

Acknowledgements	v
Abstract	vi
List of Figures	ix
List of Tables	xi
1 Introduction	1
2 Literature Review	4
2.1 LTE Cellular Networks	4
2.2 Radio Network Planning	6
2.3 Optimization under Uncertainty	7
2.3.1 Stochastic Programming	8
2.3.2 Chance-Constraint Programming	10
2.3.3 Robust Optimization	10
2.4 Related Work	11
3 Radio Network Planning under Demand Uncertainty	14
3.1 Problem Statement	14
3.2 System Model	15
3.3 Problem Formulation and Complexity	17
3.3.1 Problem Formulation	17
3.3.2 Problem Complexity	19
3.4 Results and Analysis	20
3.4.1 Tradeoff between Maximizing the Received Power and Minimizing the Number of Selected eNodeBs	21
3.4.2 RNP with Various Traffic Distributions	22
3.4.3 Comparison with Conventional RNP	25
3.5 Dynamic eNodeB Switching On/Off Strategy	26
3.6 Case Study: Football Planning Scenario	28
3.7 Summary	30

4	Radio Network Planning under Signal and Interference Level	
	Uncertainty	33
4.1	Problem Statement	33
4.2	System Model	34
4.3	Cell Edge Reliability versus Cell Area Reliability	37
4.4	Site Selection Problem	39
	4.4.1 Site Selection Problem Formulation	39
	4.4.2 Site Selection Problem Complexity	41
	4.4.3 Results and Analysis of the Site Selection Problem	43
4.5	Site Placement Problem	46
	4.5.1 Site Placement Problem Formulation	47
	4.5.2 Site Placement Problem Complexity	48
4.6	Radio Network Planning Algorithm under Uncertainty	49
	4.6.1 K-means Clustering	49
	4.6.2 Lloyd's Algorithm	50
	4.6.3 Steepest Descent Method	51
	4.6.4 Site Placement Algorithm under Uncertainty	52
	4.6.5 Radio Network Planning Algorithm under Uncertainty	53
	4.6.6 Computational Complexity	55
4.7	Results and Analysis of the Radio Network Planning Algorithm under Uncertainty	55
	4.7.1 Small Networks	56
	4.7.2 Medium to Large Networks	61
	4.7.3 Monte Carlo Simulation Results	67
4.8	Summary	68
5	Conclusions	70
A	Abbreviations	72
	Bibliography	74

List of Figures

2.1	LTE Network Architecture [1].	6
3.1	Different distributions of the active users at different times of the day for a given area.	15
3.2	The initial set of eNodeBs.	20
3.3	Six different traffic states represented in the form of user distributions in a given area.	24
3.4	The optimal subset of eNodeBs and the allocation of users to the best server after switching off selected eNodeBs during off-peak hours for (a) traffic state t_2 and (b) traffic state t_3 of case 12.	27
3.5	Six different traffic states for the movement of the football fans before and after a match of the Boca Juniors at La Bombonera stadium in Buenos Aires [2].	28
3.6	Four different traffic states of a football field represented in the form of user distributions.	29
3.7	The initial set of eNodeBs.	29
3.8	The planned area for each of the four different traffic states of a football field.	30
3.9	The planned area for each of the four different traffic states of a football field after switching off some eNodeBS at off-peak hours.	31
4.1	The effect of Rayleigh fading on the received power signal [3].	34
4.2	Cell edge reliability v/s area edge reliability [4].	38
4.3	Comparison of the cell edge reliability v/s area edge reliability curves of the new formulas with those of Reudinks [5].	39
4.4	The initial set of eNodeBs.	44
4.5	The SINR distribution of a real-life OFDMA network with a universal frequency reuse [6].	45
4.6	Coverage contours of SINR= -5 dB under a universal frequency reuse scenario [6].	45
4.7	(a) The initial distribution and (b) the planned area for a uniform distribution of UEs.	46

4.8	(a) The initial distribution and (b) the planned area for a Gaussian distribution of UEs.	46
4.9	The distribution of the UEs for case study 1.	57
4.10	The partitioned clusters and initial distribution of the eNodeBs for case study 1.	58
4.11	The initial planned area for case study 1 after solving the site selection problem.	59
4.12	(a) The contour lines of the site placement objective function and (b) the resulting planned area after moving the yellow eNodeB in the steepest descent direction of the objective function for case study 1.	59
4.13	(a) The objective function value and (b) the norm of the gradient versus the number of iterations for case study 1.	60
4.14	A semilog plot for (a) the objective function value and (b) the norm of the gradient versus the number of iterations for case study 1.	60
4.15	The resulting planned network under uncertainty for case study 1 after running the radio network planning algorithm.	61
4.16	(a) The distribution of the pixels and (b) the resulting planned network for case study 2.	61
4.17	The distribution of the pixels for case study 3.	62
4.18	The partitioned clusters and initial distribution of the eNodeBs for case study 3.	63
4.19	The distribution of the pixels for the 2 sub-networks of case study 2.	64
4.20	(a) The site selection problem result and (b) the site placement algorithm result for subnetwork 1 of case study 3.	65
4.21	(a) The site selection problem result and (b) the site placement algorithm result for subnetwork 2 of case study 3.	65
4.22	(a) The initial and (b) resulting planned network before and after running the site placement algorithm on the merged sub-networks for case study 3.	66
4.23	(a) The distribution of the pixels as well as the partitioned sub-networks (the three colors of the pixels correspond to the three partitioned sub-networks) and (b) the final planned area after solving the proposed radio network planning algorithm for the whole network of case study 4.	66
4.24	The monte carlo simulation results for the studied cases.	68

List of Tables

2.1	LTE Specification Overview.	5
3.1	The simulation parameters.	21
3.2	The selected eNodeBs for different values of α	21
3.3	Optimal subset of eNodeBs for uniform traffic states. A case represents a combination of traffic states with different probabilities of occurrence.	23
3.4	Optimal subset of eNodeBs for non-uniform traffic states. A case represents a combination of traffic states with different probabilities of occurrence.	24
3.5	Average throughput of conventional v/s stochastic RNP approach.	25
4.1	The simulation parameters.	44
4.2	The optimal subset of selected eNodeBs and the solving time for the studied cases.	47
4.3	The simulation parameters.	56

Chapter 1

Introduction

With the drastic increase in the demand, growth in mobile applications and the intense competition among different wireless cellular operators, the long term evolution (LTE), a new cellular technology, was released by the 3rd generation partnership (3GPP) in 2008 in order to get the most out of the network, meet subscriber demands and develop new revenue growth plans for the operators. LTE promises to increase network capacity, improve quality of service (QoS) and significantly enhance data rates. The main features of LTE include a flat IP-based network architecture, orthogonal frequency division multiple access (OFDMA)-based air interface, flexible bandwidth allocation (ranges between 1.4 MHz and 20 MHz), up to four times higher spectral efficiency than the state-of-the-art universal mobile telecommunications system (UMTS)/high speed packet access (HSPA) cellular technology, low latency, and support for advanced multiple input multiple output (MIMO) techniques. However, an efficient network should be designed in order to get improvements in the overall performance of the network.

Radio network planning and optimization (RNPO) is essential for operators to deploy wireless cellular networks in a cost-efficient manner. It is an essential process for operators and has a significant impact on the behavior and flexibility of the resulting network. Radio network planning (RNP) typically takes into account a geographical area, an estimated traffic load, the evolved nodeB (eNodeB) configuration and other network parameters and finds the optimal location for the eNodeBs in order to satisfy a minimum outage requirement. In conventional RNP, telecommunication networks are designed without the knowledge of actual traffic and consider a static model for the network [7–11] where the peak hour or maximum load is taken into account. Operators estimate the demand according to previous measurements and overestimate this capacity in order to cope with any future changes in the traffic volume and distribution. Moreover, the channel is considered to be deterministic and the variation in the signal and interference levels are not taken into account. However, wireless networks are characterized by many uncertain factors such as signal to interference and noise ratio (SINR)

requirements, intercell interference (ICI), traffic load and location uncertainty.

Users' location and demand have a significant effect on cellular networks performance and capacity. For instance, the location of a user equipment (UE) at different instances is an important factor that influences the SINR requirements. Besides location, traffic in mobile communications fluctuates heavily over time and thus, the cell load for an eNodeB is uncertain. Moreover, users might have different distributions at different times of the day, for example they might accumulate to a certain hotspot region due to a sports event. ICI is also a key factor in the design and implementation of wireless networks. However, interference is non-deterministic and depends on various system and channel parameters such as fading variations, frequency reuse and scheduling schemes. Therefore, a major consequence of this deterministic assumption is that it leads to performance degradation with increasing error levels. If neglected, the uncertain parameters might lead to congestion and poor performance for the resulting network. Therefore, the conventional approach leads to loss in terms of network capacities, investments, and energy and hence the need for a more realistic and accurate model of the network rises.

In this thesis, we consider the problem of the uncertain parameters present in telecommunication networks. We propose a new approach for planning an LTE network in the downlink (DL) that accounts for these parameters. The objective of our problem is to choose a minimum number of eNodeBs from an initial predefined set that still guarantees coverage, capacity and QoS requirements. A stochastic programming approach is adopted when optimizing the eNodeBs location in order to take into account the uncertainty in the number of users, their distribution, and the non-deterministic SINR. Consequently, a more realistic and accurate model of the network is provided and thus leading to a more dynamic network that has a better performance. The thesis objectives are the following:

1. Formulate a two-stage stochastic integer programming for the site selection problem for planning a network under demand uncertainty. The problem will be formulated and solved to select the minimum cardinality set of eNodeBs that satisfies the coverage and capacity requirements for the different traffic states of a given area.
2. Develop an algorithm for eNodeB switching on/off at off-peak hours in order to lower the cost and the carbon footprint of the network and thus lead to a more energy efficient wireless network operation.
3. Formulate a two-stage chance constraint optimization problem for the site selection problem taking into account the uncertainty in the signal and interference level. ICI is assumed to be non-deterministic where a semi-analytical statistical model for downlink ICI as a function of generic fading

models and scheduling schemes is adopted to illustrate the uncertainty of SINR. The problem will be formulated and solved to select the minimum cardinality set of eNodeBs that satisfies the coverage and capacity requirements for a given traffic state while maintaining the probability of outage.

4. Formulate a two-stage chance constraint optimization problem for the site placement problem taking into account the uncertainty in the signal and interference level. The objective of the formulated problem is to find the optimal locations of a fixed number of eNodeBs for a given traffic state while maintaining the probability of outage. The formulated problem will be shown to be NP-hard and thus cannot be solved.
5. Develop a site placement algorithm in order to solve the site placement problem to optimality.
6. Develop a radio network planning algorithm under uncertainty which combines the site selection optimization problem and the site placement algorithm.

This report is organized as follows. Chapter 2 provides literature review and background information on topics of direct relevance to the thesis work. Chapter 3 presents the two-stage stochastic problem formulation for planning under demand uncertainty as well as the on/off switching strategy. The site selection optimization problem, site placement optimization problem, site placement algorithm and radio network planning algorithm under the uncertainty of the signal and interference levels are given in Chapter 4. Finally, Chapter 5 provides some concluding remarks.

Chapter 2

Literature Review

The objective of this literature survey is to give a general overview about some important concepts related to the thesis work. We start by giving an overview about LTE cellular networks and radio network planning. Then, we introduce some prevailing approaches about optimization under uncertainty, where we focus on three approaches: stochastic programming (SP), robust optimization (RO) and chance-constraint programming (CCP). Finally, we investigate some previous work related to the thesis topic.

2.1 LTE Cellular Networks

LTE is the fourth generation of wireless technology that was released by 3GPP, Release 8 in 2008 as a next step after global system for mobile communications (GSM) and UMTS. Network operators are deploying 4G wireless networks to effectively deliver broadband services to a large scale of smartphone- and tablet-packing consumers eager to experience high speed applications and better offerings. LTE provides significantly increased peak data rates, with the potential for 100 Mbps in the downlink direction and 50 Mbps in the uplink (UL) direction, reduced latency, scalable bandwidth capacity, and backwards compatibility with existing GSM and UMTS technology. LTE is optimized for $0 \sim 15$ Km/h, it can support $15 \sim 120$ km/h with high performance and can also support up to 350 km/h or even up to 500 km/h. The main parameters of the LTE specifications are given in Table 2.1.

LTE uses the orthogonal frequency division multiplexing (OFDM) technology due to the high data bandwidth. Frequency resources are divided into narrow orthogonal frequency bands called subcarriers, leading to a lower data rate per subcarrier with less inter-symbol interference. Data stream of one user can be spread over several subcarriers and therefore, providing a higher overall cumulative rate and better spectral efficiency. The basic LTE resource entity is the

Table 2.1: LTE Specification Overview.

Duplex Schemes	UMTS FDD and UMTS TDD bands
Channel Bandwidth	1.4, 3, 5, 10, 15, 20 MHz
Modulation Schemes	QPSK 16-QAM, and 64-QAM (optional for handset in UL)
Access Schemes	OFDMA (DL) and SC-FDMA (UL)
DL Peak Data Rate	300 Mbps (UE category 5, 4×4 MIMO, 20 MHz)
UL Peak Data Rate	75 Mbps (20 MHz)
Latency	Idle to active less than 100 ms
Spectral efficiency	DL: $3\text{-}4 \times$ Rel 6 HSDPA, UL: $2\text{-}3 \times$ Rel 6 HSUPA
Data Type	All packet switched data
MIMO	2×2 , 4×2 , and 4×4

resource block (RB) and is of size 180 kHz in the frequency domain and 0.5 ms in the time domain. The OFDM symbols are grouped into RBs where one or more RBs can be allocated to a terminal for data transmission and reception and hence enabling the control of the total data bit-rate per terminal according to the number of RBs allocated per terminal. Since LTE supports scalable bandwidths from 1.4 MHz up to 20 MHz, then the number of RBs that can be allocated at maximum differs and ranges from 6 up to 100. Single carrier frequency division multiplexing (SC-FDMA) is used instead of OFDMA for the UL direction due to its low peak-to-average power ratio. Mobiles have power limitation and since OFDMA has high peak to average ratio, a new mode of transmission should be adopted in the UL because linear amplifiers can not be used in that case. In SC-FDMA, a single-carrier modulation and orthogonal frequency multiplexing is utilized where symbols are transmitted sequentially over one single carrier as opposed to the parallel multiple carrier transmission in OFDMA. Time-domain data symbols are transformed to frequency-domain by a discrete Fourier transform before applying the standard OFDM modulation in SC-FDMA and then applying frequency domain equalization at the receiver side.

The basic architecture of an LTE network is given in Figure 2.1. It consists of the eNodeBs, the mobility management entity (MME), the serving gateway (S-GW) and the packet data network gateway (P-GW). The eNodeBs are responsible for all radio interface-related functions (i.e. modulation/de-modulation, channel coding/de-coding) as well as other functionalities such as mobility control, user scheduling and resource allocation, power control and link adaptation, shared channel handling, hybrid automatic repeat request (HARQ), automated operation and maintenance, control and user plane security, and measurements and reporting. MME is responsible for managing mobility, user's identity and security parameters. S-GW is the node that terminates the interface towards the evolved

universal terrestrial access network (E-UTRAN). When terminals move across eNodeB in E-UTRAN, packets are routed through S-GW for intra E-UTRAN mobility and mobility with other 3GPP technologies (GSM/UMTS). P-GW is the node that terminates the interface towards the packet data network (PDN), i.e. it acts as an anchor point for sessions towards the PDN.

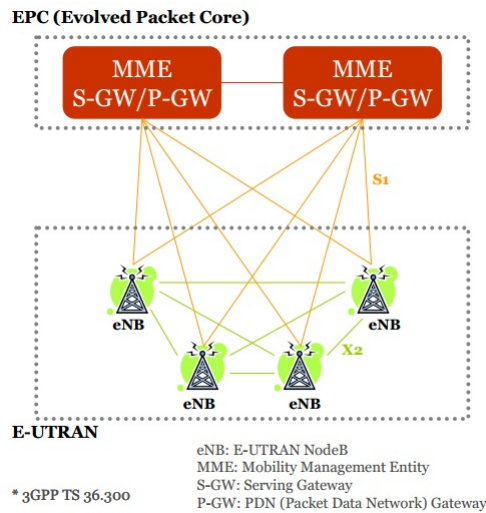


Figure 2.1: LTE Network Architecture [1].

2.2 Radio Network Planning

Radio network planning and optimization is an essential process for operators and has a significant impact on the behavior and flexibility of the resulting network. RNP typically takes into account a geographical area, an estimated traffic load, QoS requirements, blocking probability, propagation conditions, and other network parameters and finds the optimal number, location, and configuration of the eNodeBs. The main objective of RNP is to build a cellular network that provides sufficient coverage and capacity, meets the QoS requirements, and allows for flexible future system growth. A given network is said to be better if the corresponding design requires less number of network equipment and resources.

Network dimensioning is the initial phase of RNPO. It is a process through which the number of eNodeBs and their possible configurations are estimated. It includes coverage and capacity analysis. In coverage analysis, the cell range of the eNodeBs is determined and thus depends on the fading margin, cell edge target throughput, average network load as well as other parameters. The capacity analysis involves assessment of the network demand taking into account the activity

factor, UL/DL frame ratio as well as other parameters.

In order to determine the cell range and thus the number of sites needed in a given area of interest, a link budget for the connection between the eNodeB and the UE is performed for the uplink and the downlink directions. The link budget analysis (LBA) is the main tool used in coverage analysis. The target of LBA is to calculate the maximum allowed path loss (MAPL) in the signal strength, in both the uplink and downlink directions, based on an appropriate propagation model. The cell coverage range is then determined based on the MAPL, since the direction (UL or DL) with the smaller MAPL is the limiting direction if no balancing techniques are applied.

Capacity requirements take into account users' services satisfying a target QoS. In LTE, the main indicator of capacity is based on the SINR for each user. The number of required eNodeBs from the capacity analysis step is compared to that of the coverage analysis and then the larger number is used for planning.

Network planning is the second phase of RNPO. It is a process through which the optimal locations for the eNodeBs are to be determined and it is traditionally performed using professional planning tools to perform detailed predictions, for example Mentum Planet. The output of the link budget analysis is taken as a starting point and at the end of this phase, the number and location of the sites are further optimized. The planning tools typically consider a propagation model which takes into account the characteristics of the selected antenna, the terrain elevation, and the land use and land clutter surrounding each site. An elaborate traffic modeling application is employed to represent realistically users positions in the network and their different traffic profile. More detailed results are also obtained such as antenna azimuth and tilt, neighbouring and mobility parameter settings, and frequency planning where applicable.

Because of the trade-off between coverage, capacity, and service quality in an LTE network, network planning applications require an accurate simulator to provide detailed and statistically relevant information on expected network performance. Monte Carlo simulations are then carried in order to analyze the network coverage, capacity, and other vital system parameters.

2.3 Optimization under Uncertainty

Most of the approaches that have been applied in decision making have a common assumption that all the input data of the problem is known with certainty. This is known as decision making under certainty, and the corresponding models are called deterministic models. However, real life problems almost invariably include

parameters which are unknown at the time a decision should be made. "In real-world applications of linear programming, one cannot ignore the possibility that a small uncertainty in the data can make the usual optimal solution completely meaningless from practical viewpoint" - Ben-Tal and Nemirovski. Therefore, non-deterministic parameters have a significant effect on the resulting solution and hence should be considered when looking for the optimal decision. The need naturally arises to develop models that are immune to data uncertainty.

Rosenhead, Elton and Gupta (1972) divide the non-deterministic environments into two cases: risk and uncertainty. The difference between risk and uncertainty situations is that the probability distribution is known in the former case while in the uncertainty case, no information about probabilities is available. Problems in risk situations are known as stochastic programming problems where the expected value of the objective function is to be optimized. Problems under uncertainty are known as robust optimization problems and the aim is to optimize the worst-case performance of the system.

In this section, we give an overview on the approaches that can be applied to a RNP problem in order to take into account the uncertain parameters of a given network. The three approaches studied here are: stochastic programming, chance-constraint programming and robust optimization.

2.3.1 Stochastic Programming

The stochastic programming model can be viewed as an extension of the linear and nonlinear programming models to decision models where the coefficients that are not known with certainty have been given a probabilistic representation. One generally assumes that the probability distribution for the uncertainty is independent of the decisions and that the stages interact linearly. Therefore, SPs are generally modeled as recourse programs in which decisions can be taken after uncertainty is disclosed. A recourse problem is one in which only some decision variables must be fixed immediately while other variables are still unknown at this period and will be fixed at later stages. A given scenario will take into account the values that have become known in current and in previous stages, but with future stages still unknown. These postponed decisions are known as recourse variables. The goal of these problems is to optimize the first-stage decision variables so as to minimize the expected cost over other stages. Stochastic problems can be two-stage or multi-stage programs with recourse depending on the number of decisions to be taken over time as a result of different outcomes [12]. A two-stage stochastic optimization problem with recourse is defined as follows:

$$\min c^T x^0 + E_\xi Q(x^0, \xi) \tag{2.1}$$

$$\text{s.t. } Ax^0 = b \quad (2.2)$$

$$x^0 \in P \quad (2.3)$$

$$\text{where } Q(x^0, \xi) = \min q^T x' \quad (2.4)$$

$$\text{s.t. } T(x^0, x') = h \quad (2.5)$$

$$x' \in P \quad (2.6)$$

where x^0 are the first-stage variables and x' are the second stage variables. Let ξ represent the random vector which defines the constraint matrix T , cost vector q and requirement vector h after disclosing the uncertainty, and let A , c , and b define the same for the first stage. $Q(x^0, \xi)$ represents the optimal cost of the second stage for a particular scenario $\xi = (q, T, h)$ and a first-stage value of the variables x^0 . The expectation is taken with respect to ξ . P denotes additional constraints on the variables x^0 and x' .

When a finite number of scenarios exists, a two-stage stochastic linear programs can be modelled as large linear programming problems. This formulation is often called the deterministic equivalent of a stochastic program where the realizations of the random parameters are specified in the form of scenarios with the corresponding probability of each. The size of the resulting optimization model grows linearly with respect to the number of scenarios. Therefore, many methods have been proposed in order to decompose SP problems into smaller independent problems. The deterministic equivalent of a two-stage stochastic optimization problem is defined as follows:

$$\min \quad c^T x^0 + \sum_{k=1}^m p_k (q^k)^T x^k \quad (2.7)$$

$$\text{s.t. } Ax^0 = b \quad (2.8)$$

$$T^k(x^0, x^k) = h^k \quad k = 1, 2, \dots, m \quad (2.9)$$

$$(x^0, x^k) \in P \quad k = 1, 2, \dots, m \quad (2.10)$$

where m represents the finite set of scenarios. Each scenario k occurs with probability p^k and we denote the constraint matrix, cost vector and requirement vector by T^k , q^k , and h^k respectively.

2.3.2 Chance-Constraint Programming

As opposed to SP that consider the expected value of the objective function, some models require a probabilistic information about the performance of the system. There are three approaches in the literature that consider a probabilistic environment. These approaches are: max-probability locations, chance-constrained programming, and distribution maps [13]. In this section we focus on the chance-constraint approach.

Stochastic chance-constrained programming is a branch under stochastic optimization approaches that was first proposed by Charnes and Cooper. It requires the probability of a certain constraint to be satisfied with a specified probability or confidence level at the optimal solution. The general form of a CCP problem is as follows:

$$\min_x f(x)$$

$$\text{s.t. } \Pr(g_j(x, \xi) \geq \epsilon)(j = 1, 2, \dots, k) \geq (1 - \alpha) \quad (2.11)$$

$$x \in R^n \quad (2.12)$$

where x is a vector of decision variables, ξ is the stochastic vector with a given probability density function $\Phi(\xi)$, $f(x)$ is the objective function, $g(x, \xi)(j = 1, 2, \dots, k)$ are the constraint functions, $\Pr\{\cdot\}$ denotes the probability of the event $\{\cdot\}$ and $(1 - \alpha)$ is the specified confidence level of the constraint function to be satisfied. The best way to solve a CCP problem is to change the stochastic constraints to their corresponding deterministic equivalent. However, this approach is not always feasible and depends on the probability distribution function (PDF) of the stochastic constraint. Moreover, for problems that can be converted to their deterministic equivalent, it is usually difficult to convert and one can always obtain a nonlinear programming which is a hard problem. Therefore, many algorithm have been developed to solve the computation problem of the stochastic chance-constrained linear programming problems such as genetic algorithms based on stochastic simulation (see [14], [15] and [16]).

2.3.3 Robust Optimization

Robust Optimization is also an approach under uncertainty, however, the uncertainty model is not stochastic, but rather deterministic and set-based. In other words, the variable is not fixed neither random but belongs to a given set. Using this framework, we do not need any information about the probabilistic distribution of the uncertainty. Instead, a solution is said to be robust if it is feasible for all realizations of the data in the given uncertainty set. In RO, we aim at finding the cost-optimal robust solution. Similar to the case in two-stage stochastic programming, the second stage decision problem will derive recourse decisions after

the first stage decisions are made and the uncertainty is revealed.

Soyster first proposed a linear optimization model to construct a solution that is feasible for all data that belong to a convex set [17]. The resulting model produces solutions that are too conservative in the sense that we give up too much of optimality for the nominal problem in order to ensure robustness. Ben-Tal and Nemirovski addressed the issue of over-conservatism, by proposing less conservative models that consider uncertain linear problems with ellipsoidal uncertainties, which involve solving the robust counterparts of the nominal problem in the form of conic quadratic problems [18]. However, this approach leads to nonlinear, although convex, models. Therefore, Bertsimas and Sim proposed the Γ -robustness approach [19]. This approach is based on the robustness parameter Γ that can be varied in order to adapt the number of uncertain factors, that is, there is a full control on the degree of conservatism for every constraint. Unlike Ben-Tal and Nemirovski, the resulting model is linear.

2.4 Related Work

In this section, we give an overview of the work related to radio network planning. The previous work can be divided into two categories: some work that did not take into account the uncertain parameters present in the network during the planning process, and other work that considered some uncertainty aspects present in the network.

The authors in [20–22] propose discrete optimization algorithms using randomized greedy procedures and a tabu search (TS) algorithm for the uplink direction of UMTS networks. The model in [20–22] is extended in [23] to take into account signal-quality constraints in both uplink and downlink directions as well as the power control mechanism. In [8], the authors develop optimization models and algorithms for joint uplink/downlink UMTS radio network planning with SIR-based power control for UMTS networks.

In [24], the authors develop an optimization framework based on simulated annealing for site selection and BS configuration such as antenna type, power control, azimuth, and tilt. The authors in [25] investigate three nonlinear optimization algorithms—the Hooke and Jeeves method, quasi-Newton, and conjugate gradient search procedures—in order to solve the problem of finding the optimal locations of the base stations (BSs).

In [26, 27], the authors consider the problem of RNP for an energy efficient network. The authors in [26] consider a proactive approach for LTE radio network planning with green considerations that aim at finding the optimal set of eN-

odeBs and then switching on/off a subset of the selected eNodeBs based on the changing traffic conditions. In [27], the authors introduce a novel approach that jointly optimizes planning and energy management where the resulting formulated problem is tested on LTE scenarios.

Recently, uncertainty in mobile networks is becoming a main concern due to the gains that can be achieved by taking into consideration the non-deterministic parameters while planning for a more efficient network in terms of cost and performance. Many approaches have been proposed based on stochastic and robust optimization.

A stochastic model for optimizing the operator's revenue for UMTS networks is developed in [28]. The aim of this work is to maximize the expected profit given probability distributions for the peak demands in each market. The authors present a Benders' reformulation of the stochastic integer program. However, the proposed optimization formulation in [28] is not tractable, i.e., proved to be inefficient to solve; as a result, the optimal solution was not investigated and a heuristic method is developed instead.

Operators are facing the challenge to match the demand by continuously expanding and upgrading the network infrastructure. Therefore, in [29], the authors introduce a long-term network planning approach based on multistage stochastic programming, where demand evolution is considered as a stochastic process and the network is extended as to maximize the expected profit. The approach proves capable of designing large-scale realistic code division multiple access (CDMA) networks with a time-horizon of several years. Results show an increase for the expected profit by at most 18.9% as compared to the deterministic optimization.

The authors in [30] propose a basic stochastic RNP technique to the combined problem of BS location and optimal power allocation in order to deal with the expected user distributions. The problem to be solved is to place several femto-cells with much lower transceiver power budget in the same region to reduce the overall use of energy. This is achieved by allowing collaboration among the new BSs to serve the users cooperatively. However, intercell-interference is ignored in the proposed formulation.

The adjustable Γ -robustness approach of Bertsimas and Sim has been applied to network design problems [31], [32], and [33]. In [31], the authors present a model for the energy-efficient planning of wireless networks to deal with demand uncertainty for OFDMA systems. The demand values are modelled as symmetric and bounded random variables that take values in $[\bar{w}_t - \hat{w}_t, \bar{w}_t + \hat{w}_t]$. Results illustrate that their approach can lead to energy savings either by deploying less eNodeBs or serving more UEs with the same number of eNodeBs. The authors in [32]

investigate the polyhedral structure of a Γ -robust problem and present robust versions of the cutset inequalities as well as computational results on their effectiveness. In [33], the authors present three different mathematical formulations for the problem of telecommunication network design under traffic uncertainty, provide valid inequalities, study the computational implications, and evaluate the realized robustness. To enhance the performance of the mixed-integer programming solver, the authors derive robust cutset inequalities generalizing their deterministic counterparts. Furthermore, the price of robustness is studied and the approach is evaluated by analyzing the real network load.

The work in [34] presents a robust model for network design assuming that the uncertain demand belongs to a given uncertainty set. The problem to be solved is a two-stage problem where the first stage concerns the capacity planning and the second stage the routing of messages. The second stage is adaptive: the routings will be selected to match the demands using the installed capacities. Results show that the robust optimization approach leads to a decrease in the total cost as compared to the deterministic one.

Chapter 3

Radio Network Planning under Demand Uncertainty

3.1 Problem Statement

In mobile networks, traffic fluctuates heavily over time which rises uncertainty in the cell load for an eNodeB. Conventional radio network planning focuses on a static model for the traffic distribution which is usually taken at hours of peak demand. However, a major disadvantage of such a deterministic model is that the locations of the eNodeBs are not optimized for the various traffic distributions that vary across the day and hence decreases the average network's throughput or the end user's QoS at off-peak hours. In this chapter, we propose a stochastic optimization methodology to deal with the uncertainty in the users' location at different times of the day. The main contribution of this work is formulating and solving the stochastic LTE RNP problem. The aim is to deploy a cost and energy efficient LTE RNP network by minimizing the required number of eNodeBs to be installed while maximizing the SINR of the users in the network. First, we present a two-stage integer linear programming (ILP) formulation that jointly optimizes the locations of the eNodeBs and the allocation of the users to eNodeBs while meeting their target SINRs and the demand uncertainties. Then, we discuss the complexity of the problem and prove that it is NP-hard. The computational time of NP-hard problems increases with the network size, however, this is not of importance in problems that can be computed offline such as RNP problems where the eNodeBs are deployed once and for all. Thus, the operators concern is not about the computational time of the solution as much as about optimizing the performance of the network. Moreover, we extend the two-stage approach to switch off some eNodeBs during low traffic states and thus lowering the cost as well as the carbon footprint of the network. Finally, we apply the proposed formulation and the on/off algorithm to a football planning scenario.

3.2 System Model

Given a geographical area of interest on which an LTE network has to be deployed, the problem is to determine the locations where eNodeBs should be installed to guarantee coverage, capacity and QoS requirements. From a given large set of candidate locations, a subset of eNodeBs locations is chosen which are optimized for the various traffic distributions of the network at different times. For example, Figure 3.1 shows that for a given area, the distribution and location of the users as well as the traffic demand varies over time.

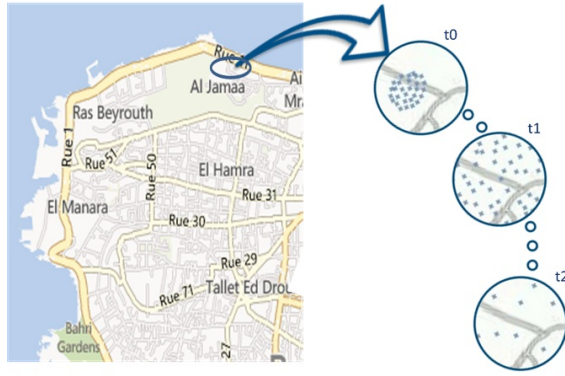


Figure 3.1: Different distributions of the active users at different times of the day for a given area.

The main parameters in the considered system model are the following:

- A set of traffic states, $\mathcal{T} = \{t : t = t_1, \dots, t_n\}$.
- A candidate set of eNodeBs, $\mathcal{I} = \{i : i = 1, \dots, N_0\}$, with cartesian coordinates (x_i, y_i) .
- Several sets of UEs, $\mathcal{K}_t = \{k : 1, \dots, K_t\} \forall t$, with cartesian coordinates (u_k, v_k) . K_t is the total number of UEs for a given traffic state t .
- The maximum number of users, N_c , that can be served by each eNodeB for downlink transmission.
- A maximum eNodeB transmit power, P_{\max} .
- A target outage probability, β .

To model uncertainty, we divide the area of interest into smaller regions called clusters. We observe the UEs' demand over different instances of the day and

pick the different distributions of the active UEs for the studied cluster. Therefore, we consider different traffic states (t) at different times of the day taking into account the probability of occurrence of every traffic state $p(t)$. Our goal is to find a solution that has the best performance under all considered states.

To decide on the eNodeB locations and the UEs they serve at various times, the following decision variables should be defined:

$$c_i = \begin{cases} 1 & \text{if eNodeB } i \text{ is deployed,} \\ 0 & \text{otherwise} \end{cases}$$

$$s_{k,i,t} = \begin{cases} 1 & \text{if UE } k \text{ in state } t \text{ is assigned to eNodeB } i, \\ 0 & \text{otherwise} \end{cases}$$

In LTE, the downlink signal to noise and interference ratio (Γ) over a given subcarrier assigned to UE k can be modeled as follows:

$$\Gamma_k = \frac{P_{k,b(k)}}{\sigma^2 + I_k} \quad (3.1)$$

where $P_{k,b(k)}$ is the received power for UE k by its serving eNodeB, σ^2 is the thermal noise power, and I_k is the intercell interference from neighboring eNodeBs. We assume that all eNodeBs are transmitting with maximum power P_{\max} and universal frequency reuse. Given that equal power allocation achieves good performance with respect to the optimal solution, we assume that the eNodeB transmits with a power of P_{\max}/N_{sub} over a given subcarrier (e.g. see [35]). Thus, the received power at UE k from eNodeB i can be expressed as:

$$P_{k,i}(\text{dB}) = 10 \log_{10} \left(\frac{P_{\max}}{N_c} \right) - L_{k,i} \quad (3.2)$$

where $L_{k,i}$ is an estimate of the pathloss between UE k and eNodeB i . It can be modeled according to TR 25.942 as follows [36]:

$$L_{k,i}(\text{dB}) = 128.1 + 37.6 \log_{10}(d_{k,i}) \quad (3.3)$$

where $d_{k,i}$ (in Km) represents the Euclidean distance between eNodeB i and UE k .

The interference term in (3.1) depends only on the intercell interference since the subcarriers are orthogonal per cell in an OFDMA-based network. For a UE to be served, it should be allocated at least one of the RBs and its downlink Γ needs

to exceed a minimum threshold value Γ_{thr} . The SINR expression can be written as follows:

$$\Gamma_k = \frac{P_{k,b(k)}}{\sigma^2 + \sum_{i=1, i \neq b(k)}^{N_0} c_i P_{k,i}} \geq \Gamma_{\text{thr}} \quad (3.4)$$

where c_i indicates whether eNodeB i is used or not. The term $\sum_{i=1, i \neq b(k)}^{N_0} c_i P_{k,i}$ represents the interference power received from neighboring eNodeBs i at UE k .

Thus, an upper bound for the downlink user spectral efficiency can be given by Shannon's capacity relation:

$$R_k(\text{bps/Hz}) = \frac{1}{2} \log_2(1 + \Gamma_k) \quad (3.5)$$

We consider only the pathloss term when modeling the physical channel since shadowing and fading are normally compensated for in RNP by adding margins to the link budget analysis depending on their anticipated effects on the received signal [37].

3.3 Problem Formulation and Complexity

In this section, we present the optimization problem formulation for LTE RNP under demand uncertainty. Then, we discuss the complexity of the problem.

3.3.1 Problem Formulation

The objective of this work is to minimize the number of eNodeBs and maximize the signal to interference noise ratio while considering the uncertainty in the traffic demand; thus, we use a stochastic programming approach in our formulation. We consider a two-stage recourse formulation where second stage decisions are regarded as corrective actions after uncertainty is disclosed. Moreover, we formulate the deterministic equivalent of the stochastic problem where the realizations of the random parameters are specified in the form of scenarios (traffic states) [12]. The two-stage decisions are as follows:

- In the first stage, the location of the eNodeBs is determined without knowing the exact distribution of the UEs in the studied area.
- In the second stage, each UE is assigned to a particular eNodeB in order to maximize Γ_k . This decision is taken after the UE distribution is revealed.

Therefore, the deterministic equivalent of the two-stage stochastic problem is formulated as follows:

$$\min_{\mathbf{s}, \mathbf{c}} \alpha \sum_{i=1}^{N_0} c_i - (1 - \alpha) \sum_{t=1}^T p(t) \sum_{k=1}^{K_t} \sum_{i=1}^{N_0} s_{k,i,t} P_{k,i,t} \quad (3.6)$$

subject to

$$\begin{aligned} & c_i P_{k,i,t} - \Gamma_{\text{thr}} \sum_{j=1, j \neq i}^{N_0} c_j P_{k,j,t} - \Gamma_{\text{thr}} \sigma^2 \\ & \geq \left(-\Gamma_{\text{thr}} \sum_{j=1, j \neq i}^{N_0} P_{k,j,t} - \Gamma_{\text{thr}} \sigma^2 \right) (1 - s_{k,i,t}) \quad \forall k, i, t \end{aligned} \quad (3.7)$$

$$s_{k,i,t} \leq c_i \quad \forall k, i, t \quad (3.8)$$

$$\sum_{i=1}^{N_0} s_{k,i,t} \leq 1 \quad \forall k, t \quad (3.9)$$

$$\sum_{k=1}^{K_t} s_{k,i,t} \leq N_c \quad \forall i, t \quad (3.10)$$

$$\sum_{k=1}^{K_t} \sum_{i=1}^{N_0} s_{k,i,t} \geq (1 - \beta) K_t \quad \forall t \quad (3.11)$$

$$s_{k,i,t} \in \{0, 1\}, c_i \in \{0, 1\} \quad (3.12)$$

The objective (3.6) represents a weighted multi-objective function that minimizes the number of eNodeBs and maximizes the average received power for each UE over the considered traffic states where α represents the weight factor. $P_{k,i,t}$ represents the received power for UE k served by eNodeB i in traffic state t . Constraint (3.7) represents the quality of service of the UEs in the network and it corresponds to the reformulation of equation (3.4) in order to have linear constraints. If $s_{k,i,t} = 1$, i.e., if UE k in traffic state t is served by eNodeB i , then this guarantees that the achieved Γ_k of UE k is greater than the required threshold Γ_{thr} as required by (3.4). Moreover, if $s_{k,i,t} = 0$, i.e., if UE k in traffic state t is not served by eNodeB i , then constraint (3.7) is feasible since the left hand side of (3.7) is always greater than or equal to its right side. Note that constraint (3.7) is redundant and thus feasible for both served and non-served UEs in the network. Constraint (3.8) can allocate UE k in traffic state t to be served by eNodeB i , i.e., $s_{k,i,t} = 1$, only if eNodeB i is selected to be on service in the network, i.e., $c_i = 1$. Constraint (3.9) forces each UE k of every traffic state t to be served by at most one eNodeB in order to maximize the number of served UEs in the network since each eNodeB has a limited capacity. Each eNodeB i can serve at most N_c users as shown in constraint (3.10). Constraint (3.11) guarantees that the percentage of users in outage, i.e., unserved users k whose $s_{k,i,t} = 0 \forall i$, is lower than the

target outage probability β for every traffic state. Finally, constraint (3.12) sets the decision variables c_i and $s_{k,i,t}$ to be binary.

3.3.2 Problem Complexity

Theorem 1. *The formulated LTE RNP problem under uncertainty is NP-hard.*

Proof. The formulated RNP problem corresponds to the stochastic capacitated facility location problem (SCFLP). To show that this problem is NP-hard, we will show that a relaxed instance of it is similar to stochastic uncapacitated facility location problem (SUFLP) which is known to be NP-hard [38].

In the deterministic uncapacitated facility location problem (FLP), we are given a set of facilities F and a set of clients D and our aim is to select a subset of facilities to open and assign each client to an open facility. Each facility i has an opening cost f_i and each client j has demand d_j and there is a cost $d_j c_{ij}$ for assigning client j to facility i where c_{ij} denotes the distance between i and j . The goal is to minimize the sum of the facility opening as well as the client assignment costs. In this problem, the demand of the clients is assumed to be deterministic, while on the other hand, the two-stage stochastic version of this problem considers the demand of the client to be a random variable and not known at the first stage and hence client j has demand d_j^k in scenario k . Each facility i has two kinds of opening cost, a first-stage opening cost of f_i^0 , and recourse costs of f_i^k in scenario k which is scenario-dependent. The objective in this case is to assign each client in each scenario to an open facility which is opened either in the first stage or in the second stage such that the total opening and assignment cost is minimized. The general formulation of the SUFL problem is given as follows [39]:

$$\min \sum_{i \in F} f_i y_i^0 + \sum_{k=1}^m p_k \left(\sum_{i \in F} f_i^k y_i^k + \sum_{i \in F, j \in D} d_j^k c_{ij} x_{ij}^k \right) \quad (3.13)$$

subject to

$$\sum_{i \in F} x_{ij}^k \geq d_j^k \quad \forall j \in D, \forall k \quad (3.14)$$

$$x_{ij}^k \leq y_i^0 + y_i^k \quad \forall i \in F, \forall j \in D, \forall k \quad (3.15)$$

$$x_{ij}, y_i \quad \text{non - negative integers} \quad (3.16)$$

The difference between SCFLP and SUFLP is that in the former case, the facilities has capacities and hence a limit on the number of clients they can serve. In SCFLP, a set of capacitated facilities is to be selected to provide service to demand points with stochastic demand. The aim is to minimize the total cost of locating facilities, in the first stage, and demand allocation under all scenarios,

in the second stage, while satisfying demand subject to facility capacities [38]. For instance, if we consider a relaxed instance of the LTE RNP problem where the SINR constraint (7) is relaxed and the outage probability β is set zero, the problem becomes exactly similar to the SCFLP which is NP-hard [38]. Thus, the more general LTE RNP problem under uncertainty is NP-hard. We can easily show that any given solution can be verified in polynomial time, thus, the general LTE RNP under uncertainty is NP-hard. \square

3.4 Results and Analysis

This section presents results and analysis for the proposed optimization framework. The proposed formulation in Section 3.3 is solved using CPLEX 12.5 on a windows 7, dual core Duo CPU P8700 @ 2.53 GHz machine. The CPLEX solver uses linear programming (LP) based branch and bound and cutting plane algorithms to solve ILP problem to optimality [40]. The initial distribution of the eNodeBs from which the optimal subset is selected is given in Figure 3.2. The general simulation parameters used throughout the different scenarios are presented in Table 3.1.

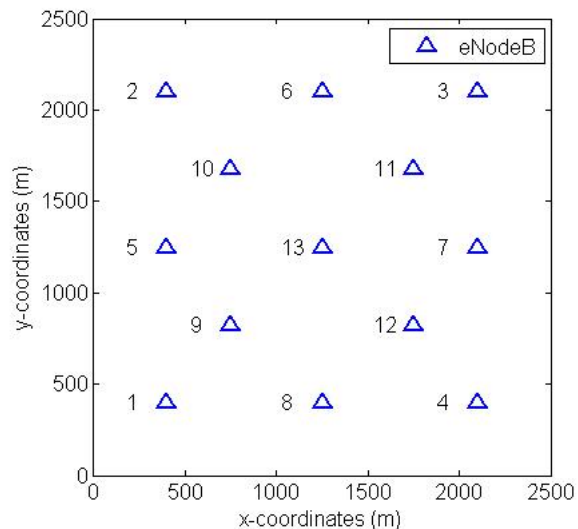


Figure 3.2: The initial set of eNodeBs.

Table 3.1: The simulation parameters.

Area size	2.5Km×2.5Km
Initial set of eNodeBs	13
Max Tx power per eNodeB	42 dBm
Bandwidth	3 MHz
Number of resource blocks	15
Noise variance	5.97×10^{-14} W
SINR threshold	-5 dB
Outage probability	0.05

3.4.1 Tradeoff between Maximizing the Received Power and Minimizing the Number of Selected eNodeBs

To study the impact of the multi-objective weight α in the objective, we consider different values for α for two cases. In the first case, 45 UEs are distributed according to a normal distribution and a uniform distribution in traffic states 1 and 2 respectively with equal probability of occurrence, i.e., $p(t_1) = p(t_2) = 0.5$. In the second case, the number of UEs is increased to 90 also assuming uniform and normal distributions with equal probability of occurrence. Table 3.2 shows the selected eNodeBs for different values of α for both cases.

Table 3.2: The selected eNodeBs for different values of α .

α	Selected eNodeBs	
	Case 1	Case 2
0	2,3,6,9,10,11,12,13	2,6,8,9,10,11,12,13
0.1	2,3,6,9,10,11,12,13	6,8,9,10,11,12,13
0.2	3,9,10,11,12,13	6,9,10,11,12,13
0.3	9,11,12,13	6,9,10,11,12,13
0.4	9,11,13	6,9,10,11,12,13
0.9	9,11,13	6,9,10,11,12,13
1	3,8,13	2,3,6,7,10,11

Taking into account the maximum number of UEs that can be served by an eNodeB, three and six eNodeBs should be selected on average for cases 1 and 2,

respectively. According to Table 3.2, when the main objective of the problem is to maximize the received power, i.e., for small values of α , the number of selected eNodeBs increases in order to decrease the effect of pathloss. However, the number of selected eNodeBs increases at most to 8 for both cases since selecting more eNodeBs increases intercell interference and therefore decreases Γ_k . In that case, Γ_{thr} would not be achieved for a number of UEs greater than the specified outage probability, and thus constraint (3.7) will no more be satisfied. Hence, there is a limit on the number of eNodeBs that can be deployed in a given area since there is a tradeoff between maximizing the received power and increasing intercell interference.

For the case where second-stage decisions are neglected, i.e., α is 1, the objective of the problem just minimizes the number of selected eNodeBs which results in a lower number of required eNodeBs compared to the case where the received power of the UEs is also maximized as demonstrated in Table 3.2. Therefore, any value of α between 0.4 and 0.9 would reduce the number of selected eNodeBs while maintaining high received power. For the following sections, we will assume that $\alpha = 0.5$.

3.4.2 RNP with Various Traffic Distributions

In this section, we consider an area having various traffic states at different instances of a day and solve the formulated problem of Section 3.3. We study the impact of the probability of occurrence, $p(t)$, of the traffic states on the set of selected eNodeBs. Several cases are studied, which are formed of a combination of the given traffic states with different probability of occurrence as shown in Tables 3.3 and 3.4. The set of resulting eNodeBs for each case is also given in Tables 3.3 and 3.4.

Uniform Traffic Distribution

In this case, we consider an area having four uniform traffic states: the first two, i.e., (t_1 and t_2), are formed of 90 users whereas the other two, i.e., (t_3 and t_4), are formed of 75 users, respectively. Table 3.3 shows the selected eNodeBs for different cases.

From Table 3.3, we deduce that the set of selected eNodeBs is different for the different cases. Case 5 is a composite of the four studied traffic states with equal probability of occurrence in order to take into account different locations of the users as well as the variation of the cell load of a given eNodeB. It is obvious that when RNP is performed taking the various traffic states across the day, a different output set of eNodeBs is obtained. The special characteristic about the obtained set is that its cardinality is equivalent to that of peak demand traffic

Table 3.3: Optimal subset of eNodeBs for uniform traffic states. A case represents a combination of traffic states with different probabilities of occurrence.

	Probability of occurrence - $p(t)$				Selected eNodeBs
	t_1	t_2	t_3	t_4	
case 1	1	0	0	0	1,3,4,9,10,11
case 2	0	1	0	0	1,2,4,5,7,11
case 3	0	0	1	0	1,4,5,10,11
case 4	0	0	0	1	3,4,5,7,9
case 5	0.25	0.25	0.25	0.25	1,3,4,5,10,11

states t_1 and t_2 which means that it minimizes the number of eNodeBs in addition to maximizing the SINR of the UEs across the day.

Non-uniform Traffic Distribution

In this case, we consider six different traffic states where users have different distribution in each. Figure 3.3 shows the distribution of the users for the considered traffic states with 90 users in traffic states t_1 and t_2 , and 40 users in traffic states t_3 , t_4 , t_5 and t_6 . Table 3.4 gives the selected eNodeBs for different probabilities for each traffic state.

In Table 3.4, cases 1 to 6 consider only one traffic state at a time and, thus, the selected eNodeBs are the closest to the distribution of active users in order to maximize the received power. Cases 7 to 13 consider multiple traffic states; therefore, the number of eNodeBs is proportional to the maximum number of active users in the studied cases in order to satisfy a given outage probability for all the considered traffic states.

In case 8, the selected eNodeBs are the ones at the corner since the considered traffic states are normally distributed at the four corners of the area. However, three eNodeBs are selected instead of four since there is a tradeoff between minimizing the set of eNodeBs and maximizing the received power.

Although cases 9, 10 and 11 consider the same traffic states, however their probabilities of occurrence are different which resulted in different sets of selected eNodeBs. For instance, the selected eNodeBs in case 9 are almost the same as case 2 since the probability of traffic state t_2 dominates while other traffic states occur only 10% of the time. Similarly, the selected eNodeBs in case 11 are the same as case 5 since traffic state t_5 occurs 70% of the time; however, three extra

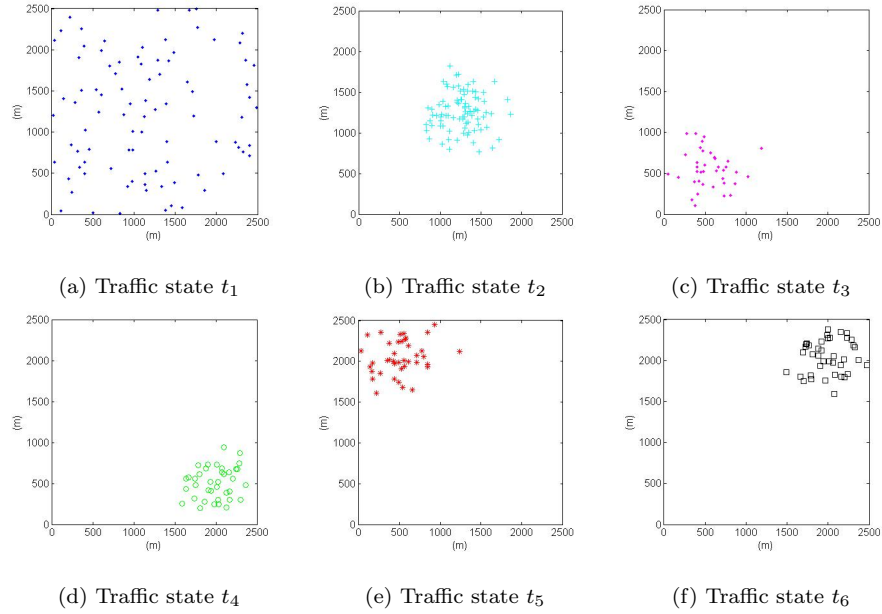


Figure 3.3: Six different traffic states represented in the form of user distributions in a given area.

Table 3.4: Optimal subset of eNodeBs for non-uniform traffic states. A case represents a combination of traffic states with different probabilities of occurrence.

	Probability of occurrence - $p(t)$						Selected eNodeBs
	t_1	t_2	t_3	t_4	t_5	t_6	
case 1	1	0	0	0	0	0	1,6,7,8,10,13
case 2	0	1	0	0	0	0	5,9,10,11,12,13
case 3	0	0	1	0	0	0	1,8,9
case 4	0	0	0	1	0	0	4,8,12
case 5	0	0	0	0	1	0	2,6,10
case 6	0	0	0	0	0	1	3,6,11
case 7	0.5	0.5	0	0	0	0	8,9,10,11,12,13
case 8	0	0	0.25	0.25	0.25	0.25	1,2,4
case 9	0	0.7	0.1	0.1	0.1	0	6,9,10,11,12,13
case 10	0	0.1	0.3	0.3	0.3	0	1,2,4,9,10,12
case 11	0	0.1	0.1	0.1	0.7	0	1,2,4,6,10,13
case 12	0	0.2	0.2	0.2	0.2	0.2	1,2,4,11,12,13
case 13	0	0.6	0.1	0.1	0.1	0.1	6,9,10,11,12,13

eNodeBs are selected in order to satisfy the outage requirement for the users in traffic state t_2 .

3.4.3 Comparison with Conventional RNP

In conventional RNP, the uncertain parameters are ignored and all the parameters are assumed to be static. Operators consider the peak demand traffic state for a given area and do RNP accordingly. Table 3.5 compares the proposed stochastic approach to the conventional one by presenting the average throughput over the considered traffic states of cases 9, 10 and 11 of Table 3.4.

Table 3.5: Average throughput of conventional v/s stochastic RNP approach.

	Conventional approach	Stochastic approach
case 9	0.33 bps/Hz	0.34 bps/Hz
case 10	0.32 bps/Hz	0.41 bps/Hz
case 11	0.33 bps/Hz	0.41 bps/Hz

Table 3.5 shows that case 9 has almost the same average throughput for both approaches since the probability of the peak demand traffic state t_3 dominates. Thus, the chosen eNodeBs for cases 2 and 9 are almost the same. However, when all the traffic states have equal probabilities, as in case 10, then higher uncertainty rises in the network and therefore the proposed stochastic RNP approach achieves an average increase in the network throughput by around 25%. Moreover, the traffic state with the higher probability highly affects the output selected set of eNodeBs. As a result, high gains will be achieved using the proposed stochastic approach, as shown in case 11, compared to conventional RNP which ignores lower traffic states since it is only based on the peak demand traffic state in the network.

Therefore, although the same number of eNodeBs are deployed, the average bit rate for the stochastic approach is either the same or greater than that of the conventional approach. Considering all the studied traffic states with different probabilities of occurrence for each, results show that the gain of the stochastic approach highly depends on the probability of the traffic states that yield the highest demands.

3.5 Dynamic eNodeB Switching On/Off Strategy

Energy efficiency in cellular networks is becoming a major issue for cellular operators. The carbon footprint of the information and communication technology (ICT) sector was estimated to be 2% in 2007 [41]. Moreover, the cellular networks contribution to the global CO₂ emission was 0.2% in 2007 and is estimated to reach 0.4% in 2020 according to a study in [42]. The eNodeBs add up to 80% of the entire network energy consumption [43]. The energy consumed at an eNodeB consists of the static energy and the dynamic energy. The static energy represents the energy required for the operation of an eNodeB and the dynamic energy represents the energy transmitted from an eNodeB to the UEs it serve. Improving the energy efficiency of the eNodeBs can significantly reduce both the operational cost and the carbon footprint. Therefore, in this section, we focus on reducing the static energy since it accounts for most of the total energy consumption in cellular networks. This can be achieved by several techniques such as using renewable energy sources for cooling the electronic equipment at the eNodeBs, deploying heterogeneous networks based on smaller cells, total or partial switching off eNodeBs and so on. In this work, we propose an efficient approach to switch off selected eNodeBs during low traffic periods, thus decreasing the energy consumption of the network.

Dynamic eNodeB on/off switching depends on the traffic state of a given area at a certain time of the day. First, we find the optimal set S of eNodeBs that satisfy all traffic states taking their probability of occurrence into account as shown in Section 3.3. Then, during the day and as the network's traffic state changes, some eNodeBs in S can be switched off at off-peak hours and then switched on as needed. The optimal subset, N_t , of eNodeBs that should be switched on can be determined by applying the two-stage formulation of Section 3.3, considering only the current traffic state t of the network and that the initial eNodeB distribution is the subset S . The remaining subset, O_t , of eNodeBs that was not selected from the subset S can be switched off. The algorithmic description is given in Algorithm 1.

To illustrate the gain of the dynamic eNodeB On/Off switching strategy, we apply Algorithm 1 on case 12 of Table 3.4 as an example. Since the highest traffic state is t_2 , then the set N_2 is the same as $S=\{1,2,4,11,12,13\}$. The sets N_3 , N_4 , N_5 and N_6 for traffic states t_3 , t_4 , t_5 and t_6 are $\{1,12,13\}$, $\{4,12,13\}$, $\{2,11,13\}$ and $\{11,12,13\}$ respectively. Therefore, eNodeBs $\{2,4,11\}$, $\{1,2,11\}$, $\{1,4,12\}$ and $\{1,2,4\}$ are switched off during traffic states t_3 , t_4 , t_5 and t_6 respectively. Figure 3.4 shows the resulting area for traffic states t_2 and t_3 after switching off the eNodeBs of the sets O_2 and O_3 during traffic states t_2 and t_3 respectively.

Algorithm 1 Dynamic eNodeB switching on/off algorithm

Input: $T = \{t : t = t_1, \dots, t_n\}$; $I = \{i : i = 1, \dots, N_0\}$; $\mathcal{K}_t = \{k : 1, \dots, K_t\} \forall t$; $\{x_i, y_i, i = 1, \dots, N_0\}$; $\{u_k, v_k, k = 1, \dots, K_t\}$.

Step 1. Solve the two-stage formulation problem and label the subset of selected eNodeBs as S .

for $t = t_1 : t_n$ {For each traffic state} **do**

Step 2. Solve the two-stage formulation problem with only one traffic state (t) where the initial distribution of eNodeBs is S . Label the subset of selected eNodeBs as N_t and the remaining eNodeBs as O_t .

Step 3. Switch off the eNodeBs of the set O_t during traffic state t .

end for

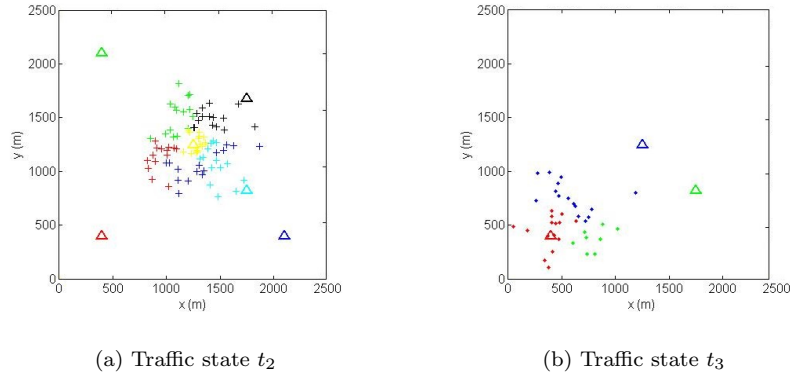


Figure 3.4: The optimal subset of eNodeBs and the allocation of users to the best server after switching off selected eNodeBs during off-peak hours for (a) traffic state t_2 and (b) traffic state t_3 of case 12.

The energy reduction gain is calculated using the following formula:

$$E_{\text{Gain}} = \sum_{t=1}^T \phi(t) \cdot C(t) \cdot P_{\text{BS}} \quad (\text{kWH/day}) \quad (3.17)$$

where $C(t)$ represents the cardinality of the set O_t for traffic state t , $\phi(t)$ denotes the number of hours per day for traffic state t , P_{BS} (in kW) is the total power (static and dynamic) consumed by an active eNodeB and ranges from 0.147 kW to 10 kW depending on the size and technology of the deployed eNodeB [44]. The energy reduction gain for the studied case is equal to $57.6 P_{\text{BS}}$ kWh/day which is equivalent to 40% gain of energy over the conventional approach.

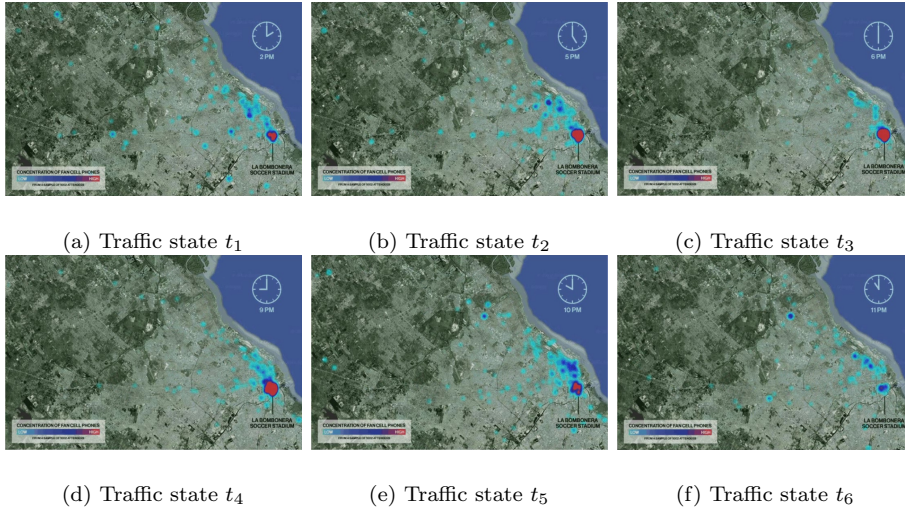


Figure 3.5: Six different traffic states for the movement of the football fans before and after a match of the Boca Juniors at La Bombonera stadium in Buenos Aires [2].

3.6 Case Study: Football Planning Scenario

In this section, we consider the case study of a green field where a stadium is to be built and we apply the formulation of Section 3.3 to plan this area. In [2], the authors show the movement of the football fans before and after a match of the Boca Juniors, a leading Argentine team, at La Bombonera stadium in Buenos Aires. After conducting a research to know which phones are fans of the Boca Juniors match, researchers tracked 1,002 of these phones as the owners converged at La Bombonera stadium and then as they made their way back home. Figure 3.5 shows the the distribution of the fans at different times of the day where the red spots indicate a higher density of fans and the blue spots reflect a lower density of fans.

In our example, we consider four different traffic scenarios of an area where a football field is to be built as shown in Figure 3.6. The number of users for the considered traffic states t_1 , t_2 , t_3 , and t_4 is 55, 90, 100 and 137 UEs respectively. Traffic states t_1 , t_2 , t_3 , and t_4 occur with a probability of $\frac{18}{24}$, $\frac{2}{24}$, $\frac{2}{24}$ and $\frac{2}{24}$ respectively. The area size is 700 m \times 700 m and the stadium size is 250m \times 160m. Moreover, we assume initially a set of 14 eNodeBs from which the optimal set is selected as shown in Figure 3.7. The max number of UEs that can be served by an eNodeB is 25 and the remaining parameters are the same as those given in Table 3.1.

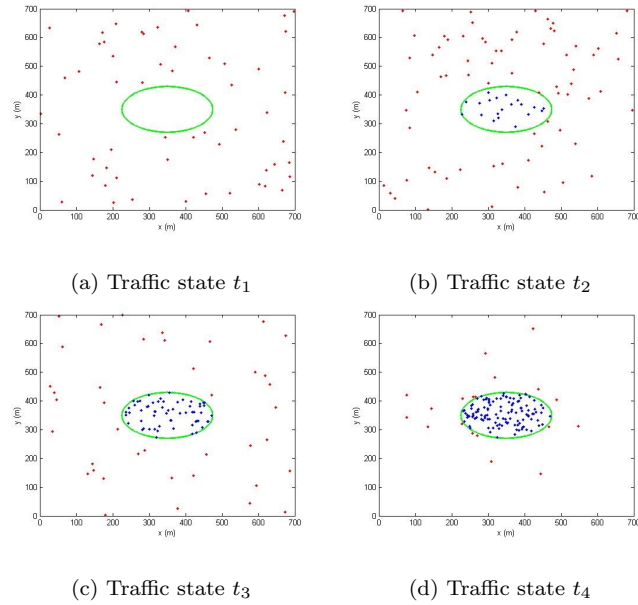


Figure 3.6: Four different traffic states of a football field represented in the form of user distributions.

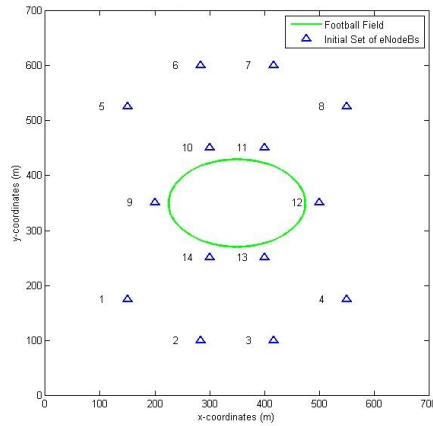


Figure 3.7: The initial set of eNodeBs.

The conventional approach consists of planning the area according to the highest traffic state i.e. t_4 . And hence the subset of selected eNodeBs is $\{9,10,11,12,13,14\}$ in that case. However, according to the stochastic approach, all the traffic states of a given area are taken into account during planning and the subset of selected eNodeBs is $\{1,4,6,8,10,13\}$. An increase in the network throughput by approx-

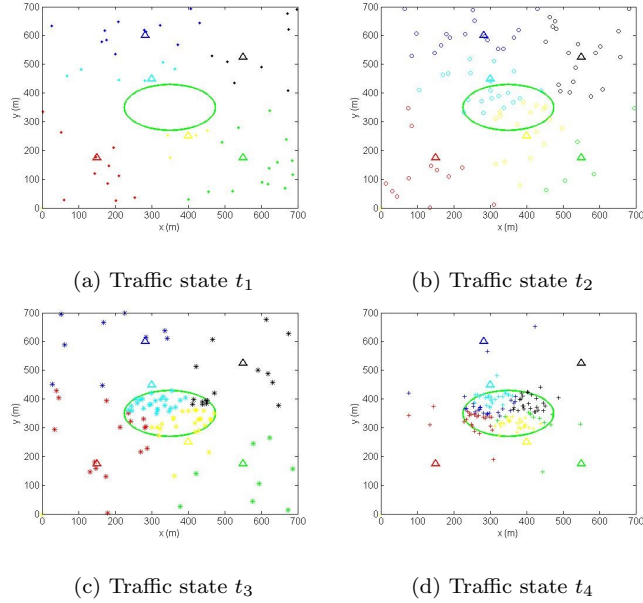


Figure 3.8: The planned area for each of the four different traffic states of a football field.

imately 35% is achieved upon applying the stochastic approach. The resulting assignment problem of the four studied traffic states, according to the stochastic approach, is given in Figure 3.8. We further apply the dynamic on/off algorithm to the resulting planned area according to the stochastic approach and hence a gain of $62 \times P_{BS}$ is achieved which is equivalent to 43% gain of energy over the conventional approach that consists of switching On all eNodeBs irrespective of the traffic state. The resulting planned area for each of the four traffic states after applying the dynamic on/off algorithm is given in Figure 3.9.

3.7 Summary

In conventional RNP, the uncertain parameters are ignored and all the parameters of a network are assumed to be static. Operators consider the peak demand traffic state for a given area and perform RNP, accordingly. In this chapter, we have presented a stochastic approach for planning a network where the randomness in the location and number of users is taken into account. Moreover, we have applied an On/Off strategy for switching off some of the eNodeBs during low traffic states.

The typical operator's aim is to optimize the network according to coverage and

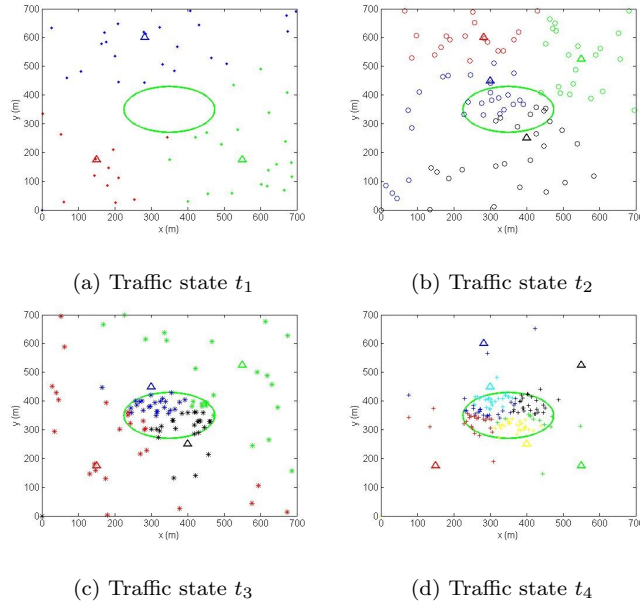


Figure 3.9: The planned area for each of the four different traffic states of a football field after switching off some eNodeBS at off-peak hours.

capacity. Call drop rates give a first indication for areas with insufficient coverage, traffic counters identify capacity problems. Therefore, the use of the stochastic approach, as illustrated in this chapter, allows the following objectives to be achieved as compared to the traditional approach:

- Providing better coverage in the network area. This objective requires that in the area, where LTE system is offered, users can establish and maintain connections with acceptable or default service quality, according to the operators requirements. The stochastic approach aims at planning a given area taking into account all the traffic states and thus allows better coverage for different traffic states. Moreover, in the given approach, the capacity of an eNodeB is fixed and the planning is done for coverage. It implies therefore that the coverage is continuous and users are unaware of cell borders and changes according to the traffic state.
- Providing better capacity in the network area. Capacity in a given network could be improved through interference reduction by switching off those cells which are not needed for low traffic states.
- Reducing energy consumption. This objective is achieved by switching-off some eNodeBs at low traffic states and therefore, making the network greener.

- Reducing the operational cost and thus reducing the operational expenditure (OPEX) of a given operator. A typical critical cost for the operator is the energy expenses. Cuts on energy expenses could be realized if the capacity offered by the network would match the needed traffic demand at any point of time as close as possible.

Chapter 4

Radio Network Planning under Signal and Interference Level Uncertainty

4.1 Problem Statement

Intercell interference is a primary factor in the design and implementation of wireless cellular networks and plays an important role between capacity and coverage tradeoff. The conventional approach for radio network planning does not directly capture the signal and interference variation due to the scheduling algorithm and fading. Therefore, a major disadvantage of such a deterministic model is that multipath fading contributes to the unreliability of wireless links, therefore, causing large deviations from link quality predictions based on path loss models. Figure 4.1 shows the effect of fading on the received signal power where the fading is assumed to be Rayleigh with a maximum Doppler shift of 100 Hz. In this chapter, we consider a new approach for optimizing LTE cellular planning where the uncertainty in the signal and interference levels is taken into account. ICI is assumed to be non-deterministic where a semi-analytical statistical model for downlink ICI as a function of generic fading models and scheduling schemes is adopted in order to illustrate the uncertainty of SINR. Maintaining the outage probability of each user below a predefined level under the interference uncertainty requires the formulation of a stochastic problem. However, we adopt a chance-constraint programming approach in order to reformulate the problem in a deterministic setting where the fading parameter is modeled as a random variable (RV). First, we present the chance-constraint formulation for the site selection problem that jointly optimizes the locations of the eNodeBs and the allocation of the users to eNodeBs while meeting a probabilistic target SINR assuming a Rayleigh fading channel. We show that the optimal solution to the problem becomes difficult to find as the size of the network increases due to the

limitation on the computational time and memory space. Second, we formulate a site placement chance constraint optimization problem for LTE RNP that aims at optimizing the locations of a set of eNodeBs taking into account the uncertainty in the signal and interference level. However, the formulated problem is shown to be NP-hard and a site placement algorithm is developed in order to solve the problem to optimality. Finally, we provide a general optimization framework for LTE RNP by developing a radio network planning algorithm under uncertainty that combines the site selection optimization problem and site placement algorithm in order to find the minimum set of eNodeBs as well as their optimal locations. Simulation results prove the optimality convergence of the algorithm and hence ensure a reliable network planning under uncertainty.

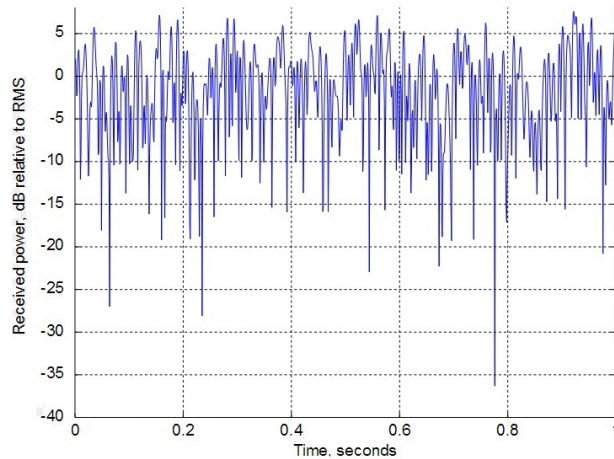


Figure 4.1: The effect of Rayleigh fading on the received power signal [3].

4.2 System Model

Given a geographical area of interest on which an LTE network has to be deployed, the problem is to determine the locations where eNodeBs should be installed to guarantee coverage, capacity and QoS requirements. For the site selection problem, a subset of eNodeBs locations from a given large set of candidate locations is chosen, and for the site placement problem, the optimal location of eNodeBs is chosen, while satisfying a minimum outage probability under uncertainty. We consider a single carrier in an OFDMA-based downlink network scenario where the main parameters in the considered system model are the following:

- A candidate set of eNodeBs, $\mathcal{I} = \{i : i = 1, \dots, N_0\}$, with cartesian coordinates (x_i, y_i) .

- A set of users, $\mathcal{K} = \{k : 1, \dots, K\}$, with cartesian coordinates (u_k, v_k) .
- The maximum number of users, N_c , that can be assigned to each eNodeB for downlink transmission.
- A maximum eNodeB transmit power, P_{\max} , that is assumed to be constant.
- A target outage probability, ϵ .

For a UE to be served, the downlink signal to interference and noise ratio (Γ) needs to exceed a minimum threshold value (Γ_{thr}). The downlink SINR for a UE k at location (u, v) is modeled as follows:

$$\Gamma(u, v) = \frac{P_{k,b(k)}}{\sigma^2 + \sum_{i=1, i \neq b(k)}^{N_0} c_i P_{k,i}} \quad (4.1)$$

where c_i indicates whether eNodeB i is deployed or not. $P_{k,b(k)}$ is the received power for UE k by its serving eNodeB, σ^2 is the thermal noise power and the term $\sum_{i=1, i \neq b(k)}^{N_0} c_i P_{k,i}$ represents the interference power received from neighboring eNodeBs i at UE k .

However, the received power as well as the interference power are non-deterministic parameters and hence the SINR is non-deterministic. Therefore, we consider in our model the uncertainty in the signal and interference levels and hence we rely on a statistical model for SINR. The composite fading is represented via the random variable A which behaves according to a PDF $f_A(a)$. We assume that the fading statistics are the same among the users and it remains constant within each symbol duration. We denote by P_i the power allocated at the eNodeB of cell i , $1 \leq i \leq N_0$. Let $\xi_i = 10^{K_i/10} \cdot P_i \cdot d_0^{\alpha_i}$ denote the composite power at the eNodeB of cell i , where α_i is the pathloss exponent and K_i in dB is the pathloss constant for the channel between cell i and the corresponding UE at location (u, v) . The channels are assumed to be subject to additive white Gaussian noise (AWGN), independent fading statistics A_i and pathloss of the form $\delta_{i,k}^{-\alpha_i}$, $\delta_{i,k}$ being the distance between the eNodeB of cell i and UE k .

Considering a UE at location (u, v) , we are interested in modeling its SINR PDF due to the interfering cells. The received power from the serving eNodeB i in equation (4.1) can be expressed as $\xi_i \delta_{i,k}^{-\alpha_i} A_i$ and the total interfering power I_{total} can be expressed as:

$$I_{\text{total}} = \sum_{j=1, j \neq i}^{N_0} I_{j,k} A_j = \sum_{j=1, j \neq i}^{N_0} \xi_j \delta_{j,k}^{-\alpha_j} A_j \quad (4.2)$$

The general expression of the SINR PDF according to [45] is given as follows:

$$f_{\Gamma}(\gamma|(u, v)) = \int_0^{\infty} \frac{\sigma^2 + \eta}{\xi_i \delta_{i,k}^{-\alpha_i}} f_A\left(\frac{(\sigma^2 + \eta)\gamma}{\xi_i \delta_{i,k}^{-\alpha_i}}\right) f_{I_{\text{total}}}(\eta) d\eta \quad (4.3)$$

where $f_{I_{\text{total}}}(\cdot)$ is the distribution of the total interfering power, f_A is the distribution of the fading, σ^2 is the additive noise power, (u, v) represents the coordinates of the UE, and $\xi_i \delta_{i,k}^{-\alpha_i}$ is the received power for a UE by its serving eNodeB.

Assuming Rayleigh channels with unity fading power, then the distribution of the fading is $f_{A_i}(a) = e^{-a}$. Therefore, the distribution of $I_{j,k}A_j$ is $f_{I_{j,k}A_j}(a) = e^{-\frac{a}{I_{j,k}}}$. Knowing that I_{total} is the sum of $(N_0 - 1)$ independent RVs, then the distribution of I_{total} is the distribution of the sum of these RVs. Moreover, the distribution of the sum of RVs is equivalent to the convolution of each distribution of the $(N_0 - 1)$ RVs. Hence, I_{total} is the convolution of $(N_0 - 1)$ distributions. To avoid convolution, we go to the frequency domain and consider the moment generating function (MGF) of I_{total} . Evaluating the MGF is a standard procedure for calculating the PDF of sums of independent RVs and therefore, we adopt this procedure for deriving the SINR PDF. Due to the independence of the A_j 's, $\text{MGF}_{\text{total}}$ can be expressed as:

$$\text{MGF}_{\text{total}}(s) = \prod_{j=1, j \neq i}^{N_0} \text{MGF}_j(s) \quad (4.4)$$

And since the MGF(s) of $I_{j,k}A_j$ is $\frac{1}{1 - I_{j,k}s}$, then the $\text{MGF}_{I_{\text{total}}}$ can be expressed as follows:

$$\text{MGF}_{I_{\text{total}}}(s) = \prod_{j=1, j \neq i}^{N_0} \frac{1}{1 - I_{j,k}s} \quad (4.5)$$

Therefore, the distribution of I_{total} is the inverse of its MGF. Hence, we simplify the expression of the MGF by applying partial fraction expansion:

$$\text{MGF}_{I_{\text{total}}}(s) = \sum_{j=1, j \neq i}^{N_0} \frac{t_j}{1 - I_{j,k}s} \quad (4.6)$$

where $t_j = \prod_{p=1, p \neq i, p \neq j}^{N_0} \frac{1}{1 - \frac{I_{p,k}}{I_{j,k}}}$. Therefore, the distribution of I_{total} given by inverting $\text{MGF}_{I_{\text{total}}}(s)$ is:

$$f_{I_{\text{total}}}(a) = \sum_{j=1, j \neq i}^{N_0} \frac{t_j}{I_{j,k}} \cdot e^{-\frac{a}{I_{j,k}}} \quad (4.7)$$

where $a \geq 0$. Let $y = \sigma^2 + I_{\text{total}}$, therefore, the distribution function of y is:

$$f_y(a) = \sum_{j=1, j \neq i}^{N_0} \frac{t_j}{I_{j,k}} \cdot e^{\frac{-a}{I_{j,k}}} \cdot e^{\frac{\sigma^2}{I_{j,k}}} \quad (4.8)$$

where $y \geq \sigma^2$. Let $z = \frac{A_i}{y}$, therefore, the distribution function of z is:

$$f_z(z) = \int_n^\infty y \cdot f_{A_i}(yz) \cdot f_Y(y) dy \quad (4.9)$$

and $\text{SINR} = \xi_i \cdot \delta_{i,k}^{-\alpha} \cdot z$, therefore, the distribution function of Γ is:

$$f_\Gamma(\gamma) = \frac{\delta_{i,k}^\alpha}{\xi_i} \cdot f_z\left(\frac{\delta_{i,k}^\alpha \gamma}{\xi_i}\right) \quad (4.10)$$

Hence, the SINR PDF can be described as follows:

$$f_\Gamma(\gamma|(u, v)) = \sum_{j=1, j \neq i}^{N_0} \left(\frac{a \cdot t_j}{I_{j,k}} \cdot \frac{e^{-a\gamma}}{b\gamma + \frac{1}{I_{j,k}}} + \frac{b \cdot t_j}{I_{j,k}} \cdot \frac{e^{-a\gamma}}{(b\gamma + \frac{1}{I_{j,k}})^2} \right) \quad (4.11)$$

where $a = \frac{\sigma^2}{\xi_i \cdot \delta_{i,k}^{-\alpha}}$ and $b = \frac{1}{\xi_i \cdot \delta_{i,k}^{-\alpha}}$.

The cumulative distribution function (CDF) of the SINR is:

$$F_\Gamma(\gamma|(u, v)) = e^{\frac{-\sigma^2 \delta_{i,k}^\alpha \gamma}{\xi_i}} \cdot \xi_i \cdot \sum_{j=1, j \neq i}^{N_0} \left(\frac{-t_j}{\xi_i + \delta_{i,k}^\alpha \gamma I_{j,k}} \right) \quad (4.12)$$

4.3 Cell Edge Reliability versus Cell Area Reliability

A major design criteria of wireless cellular networks is the radio frequency (RF) coverage. RF coverage is expressed in terms of coverage probability due to the randomness of the fading variable and hence, a link budget is required in that case. The output of the link budget analysis specifies the link margin that guarantees QoS at the cell edge. However, the reliability of RF coverage is commonly based on two measures: the cell edge reliability and the cell area reliability. The former denotes the probability that the RF signal of a UE will be above a specified threshold value at the cell edge. On the other hand, the cell area reliability is the probability that the RF signal of a UE will be above a specified threshold value after integrating the contour probability over all the contours including the cell

edge. For example, Equation (4.13) shows the derivation of the area coverage probability in case of a single cell [46].

$$P_a = \int_0^{2\Pi} \int_0^R P_{\text{cov}}(r)p(r, \varphi)drd\varphi \quad (4.13)$$

where $P_{\text{cov}}(r)$ is the coverage probability within a certain distance r , and $p(r, \varphi)$ is the distribution of the users in the cell.

Hence, the need for mapping from the cell edge coverage probability to the cell area coverage probability is a crucial step in link budgets for cellular wireless network dimensioning and designs. Reudink's formula is the most commonly adopted formula for such mapping and is adopted by many engineering books and training courses [47]. Reudink showed that there is a deterministic relationship between the two terms as shown in Figure 4.2 [4]. This relationship is determined by the ratio σ/B where σ is the standard deviation of the log-normal fading within the cell and B is the pathloss exponent. A typical value for the pathloss exponent in macrocell environment is 3.52 and for the standard deviation is 8 dB. Therefore, the ratio σ/B is 2.27 and hence, a cell edge coverage probability of 75% corresponds to a cell area probability of 90% according to Reudink's formula. Note that increasing the cell edge reliability is equivalent to decreasing the coverage radius of the cell.

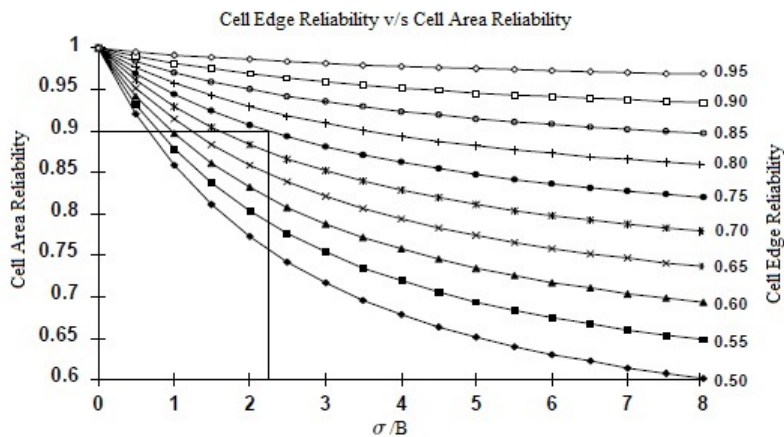


Figure 4.2: Cell edge reliability v/s area edge reliability [4].

A recent study in [5] derives new formulas for computing the area coverage probability of a cellular wireless network based on its edge coverage probability. The author shows that the disadvantage of Reudink's relationship is that it considers

the cell to be isolated. Therefore, the new formulas take into account the correlation between two fading handoff links, and allow the parameters σ and B to be different for the two fading handoff paths. Figure 4.3 shows an example for the comparison between the new derived formulas and that of Reudink where ρ is the correlation coefficient of two shadow fadings, $L_h = H_h/\sigma$, H_h is the hard handoff hysteresis, i.e., the candidate signal has to be H_h dB higher than the host signal for hard handoff to happen, and σ is the standard deviation of the shadow fading.

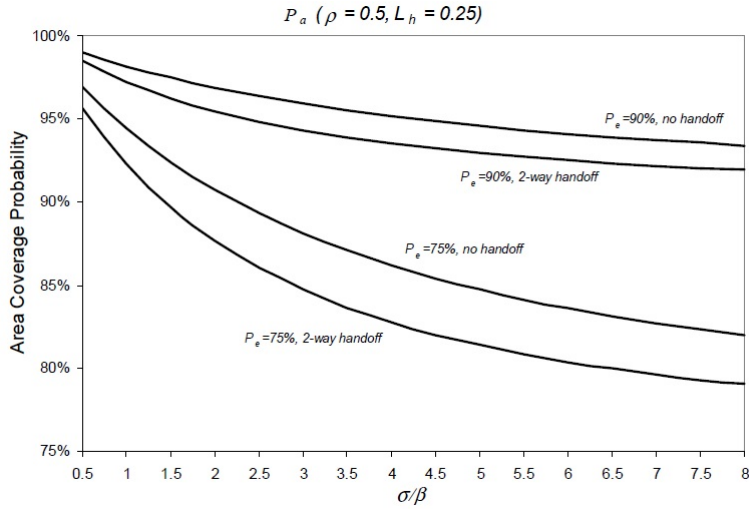


Figure 4.3: Comparison of the cell edge reliability v/s area edge reliability curves of the new formulas with those of Reudinks [5].

4.4 Site Selection Problem

In this section, we present the site selection problem formulation for LTE RNP under uncertainty. We discuss the complexity of problem, and then provide results and analysis for the proposed optimization problem.

4.4.1 Site Selection Problem Formulation

The objective of our problem is to minimize the number of eNodeBs to be deployed in a particular area and guarantee that the target threshold SINR for each UE is satisfied with a minimum probability ϵ . Therefore, we adopt a chance-constraint approach for formulating the optimization problem and we change the stochastic constraints to their corresponding deterministic equivalent. The chance-constraint approach has been used for different applications in wireless

communications. For instance, the authors in [48] develop a chance-constraint approach for the problem of power allocation in multiple input single output (MISO) networks. In [49], the authors apply the chance-constraint approach to the problem of resource allocation in order to deal with the uncertainty in the channel for OFDMA cognitive networks. To decide on the eNodeB locations, we define the following decision variables:

$$c_i = \begin{cases} 1 & \text{if eNodeB } i \text{ is deployed,} \\ 0 & \text{otherwise} \end{cases}$$

$$s_{k,i} = \begin{cases} 1 & \text{if UE } k \text{ is assigned to eNodeB } i, \\ 0 & \text{otherwise} \end{cases}$$

Therefore, the site selection optimization problem for LTE RNP under uncertainty is given as follows:

$$\min_{c,s} \sum_{i=1}^{N_0} u_i c_i - \lambda \sum_{i=1}^{N_0} \sum_{k=1}^K s_{i,k} P_{i,k} \quad (4.14)$$

subject to

$$e^{\frac{-\sigma^2 \delta_{i,k}^\alpha \Gamma_{\text{thr}}}{\xi_i}} \xi_i \sum_{j=1, j \neq i}^{N_0} \frac{c_j}{(\xi_i + \delta_{i,k}^\alpha I_{j,k} \Gamma_{\text{thr}}) (\prod_{p=1, p \neq i, p \neq j}^{N_0} (1 - \frac{c_p I_{p,k}}{I_{j,k}}))} \geq (1 - \epsilon) s_{i,k} \quad \forall i, k \quad (4.15)$$

$$s_{i,k} \leq c_i \quad \forall i, k \quad (4.16)$$

$$\sum_{i=1}^{N_0} s_{i,k} = 1 \quad \forall k \quad (4.17)$$

$$\sum_{k=1}^K s_{i,k} \leq N_c \quad \forall i \quad (4.18)$$

$$c_i \in \{0, 1\}, s_{i,k} \in \{0, 1\} \quad (4.19)$$

The objective (4.14) represents a weighted multi-objective function that minimizes the number of eNodeBs and maximizes the average received power for each UE where λ represents the weight factor that gives equal weights for both objectives since the first one is of a higher order than the second. $P_{i,k}$ represents the received power for UE k served by eNodeB i and u_i represents the cost for deploying eNodeB i . Constraints (4.15) are the probabilistic constraints and represent the QoS in the network. These constraints correspond to $\Pr\{\Gamma_{k,i} \geq \Gamma_{\text{thr}}\} \geq (1 - \epsilon) s_{i,k}$ and therefore guarantee that the probability of SINR of UE k greater than a target threshold value (Γ_{thr}), is greater than $(1 - \epsilon)\%$. The probability that the SINR

of UE k , served by eNodeB i , being greater than a threshold value is derived from the CDF expression of equation (4.12) and is given as follows:

$$\Pr\{\Gamma_{k,i} \geq \Gamma_{\text{thr}}\} = e^{\frac{-\sigma^2 \delta_{i,k}^\alpha \Gamma_{\text{thr}}}{\xi_i}} \xi_i \cdot \sum_{j=1, j \neq i}^{N_0} \frac{1}{(\xi_i + \delta_{i,k}^\alpha I_{j,k} \Gamma_{\text{thr}}) (\prod_{p=1, p \neq i, p \neq j}^{N_0} (1 - \frac{I_{p,k}}{I_{j,k}}))} \quad (4.20)$$

Therefore, according to constraint (4.15), if $s_{i,k} = 1$, i.e., if UE k is served by eNodeB i , then this guarantees that the probability that $(\Gamma_k \geq \Gamma_{\text{thr}})$ is greater than or equal to $(1-\epsilon)$. If $s_{i,k} = 0$, i.e., if UE k is not served by eNodeB i , then the right hand side is set to zero, and constraint (4.15) is feasible. Note that constraints (4.15) are redundant and non-linear. Constraints (4.16) can allocate UE k to be served by eNodeB i , i.e. $s_{i,k} = 1$, only if eNodeB i is selected to be on service in the network i.e. $c_i = 1$. Constraints (4.17) ensures that every UE in the network is served by exactly one eNodeB in order to maximize the number of served UEs since each eNodeB has a limited capacity. Each eNodeB i can serve at most N_c UEs as shown in constraints (4.18). Finally, constraints (4.19) set the decision variables c_i and $s_{i,k}$ to be binary.

4.4.2 Site Selection Problem Complexity

The formulated site selection LTE RNP problem under uncertainty is NP-hard. The problem type is nonlinear integer program (NIP), it involves nonlinear inequality constraints (4.15). If we restrict our model to contain only linear functions, NIP reduces to an ILP, which is an NP-hard problem. On the other hand, if we restrict our model to have no integer variable but allow for general nonlinear functions in the objective or the constraints, then NIP reduces to a nonlinear program (NLP) which is also known to be NP-hard [50]. Hence, the determination of a global solution to our problem is NP-hard.

Moreover, the formulated problem corresponds to a chance-constrained approach of a capacitated facility location problem (CFLP) [38]. Chance-constrained programming involves requiring the probability of a certain constraint holding to be sufficiently high [38]. In CFLP, a set of capacitated facilities is to be selected to provide service to demand points. The aim is to minimize the total cost of locating facilities, in the first stage, and demand allocation, in the second stage, while satisfying demand subject to facility capacities [38]. Let $I = 1, \dots, M$ be the set of customers to be served by the selected plants from the potential set $J = 1, \dots, N$. Each selected site is denoted by j . The cost of opening a site is f_j and the cost of assigning customer i to plant j is r_{ij} . $X_{ij} = 1$ indicates whether facility j serves customer i whereas $X_{ij} = 0$ indicates otherwise. $Y_j = 1$ indicates whether facility j is opened whereas $Y_j = 0$ indicates otherwise. The general formulation

of a CFLP problem is given as follows [26]:

$$\min_{X,Y} \sum_{j=1}^N f_j Y_j + \sum_{i=1}^M \sum_{j=1}^N r_{i,j} X_{i,j} \quad (4.21)$$

subject to

$$\sum_{j=1}^N X_{i,j} = 1 \quad \forall i \quad (4.22)$$

$$X_{i,j} \leq Y_j \quad \forall i, j \quad (4.23)$$

$$\sum_{j=1}^N a_i X_{i,j} \leq b_j Y_j \quad \forall i \quad (4.24)$$

$$Y_i \in \{0, 1\}, X_{i,j} \in \{0, 1\} \quad (4.25)$$

- The objective 4.21 minimizes the cost of opening facilities as well as the cost of assigning customers to the opened facilities.
- Constraint 4.22 ensures that each customer is assigned only to one facility.
- Constraint 4.23 allocates customer i to be served by facility j , i.e. $X_{i,j} = 1$, given that facility j is an open facility, i.e., $Y_j = 1$.
- Constraint 4.24 ensures that the customer's demand is less than or equal to the facility's capacity.
- Constraint 4.25 sets the decision variables $X_{i,j}$ and Y_j to be binary.

To show that the formulated RNP problem is NP-hard, we will also prove that a relaxed instance of it is similar to the CFLP which is known to be NP-hard. The objective (4.14) corresponds to objective (4.21). Moreover, constraints (4.16), (4.17), (4.18), and (4.19) correspond to constraints (4.23), (4.22), (4.24), and (4.25) respectively. If we consider a relaxed instance of the LTE RNP problem where the QoS constraints (4.15) is relaxed, the problem becomes exactly similar to the CFLP which is NP-hard.

A relaxed version of our problem is proven to be at least as hard as the CFLP which is NP-hard. Thus, the more general LTE RNP problem under uncertainty is NP-hard. We can easily show that any given solution can be verified in polynomial time, thus, the general LTE RNP under uncertainty is NP-hard.

4.4.3 Results and Analysis of the Site Selection Problem

In this section, we present results and analysis for the proposed optimization framework. Methods that have addressed the solution of an NIP include the branch and bound method (BB), generalized benders decomposition (GBD), outer-approximation (OA), LP/NLP based branch and bound, and extended cutting plane method (ECP). However, the most common approach is the branch-and-bound method [50]. Therefore, we solve the proposed site selection optimization problem using the branch-and-reduce optimization navigator (Baron) 11 solver with CPLEX as LP solver and MINOS as NLP solver. The Baron solver is a global optimization (GO) solver that can solve non-convex optimization problems to global optimality. Purely continuous, purely integer, and mixed-integer nonlinear problems can be solved with Baron. It tries to find convex under-estimators for the nonlinear functions, i.e. it replaces each non-convex function $f_j(x, y)$ with a convex function $g_j(x, y)$ such that $g_j(x, y) \leq f_j(x, y)$ for all (x, y) in the domain of interest. Another way is to define a new variable, for example, z_j , which acts as a place holder for $f_j(x, y)$, and to add constraints which force z_j to be approximately equal to $f_j(x, y)$. In this latter approach, one adds constraints of the form $z_j \leq g_j(x, y)$, where $g_j(x, y)$ is again a convex under-estimator [50]. However, for our formulated problem, the under-estimator for the function of constraint (4.15) is weak and it requires much nodes to find a good under-estimator, and therefore takes a lot of time. Therefore, we implement our problem on small to medium sized networks.

We perform simulations on a windows 7, dual core Duo CPU P8700 @ 2.53 GHz machine. We assume that all eNodeBs are transmitting with the maximum transmit power. Given that equal power allocation achieves good performance with respect to the optimal solution, we assume that the power is equally allocated among the UEs in the network (e.g. see [35]). The general simulation parameters used throughout the different scenarios are presented in Table 4.1. The initial set of eNodeBs from which the optimal subset is selected is given in Figure 4.4

An outage probability of at most (ϵ) 25% corresponds to a cell edge reliability of 75%. Therefore, according to Section 4.3, this value corresponds to cell area reliability of 90%. Moreover, in our problem, we assume a universal frequency reuse, and hence high levels of interference and low SINR can be expected near the cell edge. The authors in [6] show the SINR distribution of a real-life OFDMA network and reveal that the SINR can reach -12 dB for the cell edge users as shown in Figure 4.5. Moreover, consider the best-case scenario, where SINR $= -5$ dB is needed to avoid radio link failure. Figure 4.6 shows the results from 3GPP-like modeling where even in such an idealistic network, under the best-case scenario SINR $= -5$ dB contours cannot reach the cell edge with 75% of cell-edge reliability [6]. Therefore, we use in our simulations an SINR threshold of -7 dB.

Table 4.1: The simulation parameters.

Area size	1.5Km×1.5Km
Initial set of eNodeBs	13
Max Tx power per eNodeB	42 dBm
Bandwidth	3 MHz
Antenna gain	11 dBi
Cable, connector, and combiner losses	2.5 dB
Max number of UE served by an eNodeB	15
Noise variance (σ^2)	5.97×10^{-14} W
SINR threshold (Γ_{thr})	-7 dB
Percentage of outage (ϵ)	0.25
Pathloss constant (K)	-80dB
Pathloss exponent (α)	2
Reference distance (d_0)	1

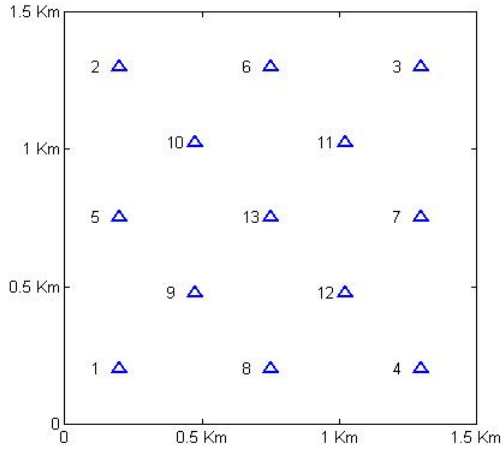


Figure 4.4: The initial set of eNodeBs.

We consider small sized networks for our simulation results. Two cases are studied where in the first case, 25 UEs are distributed uniformly in the area while in the second case 36 UEs with a Gaussian distribution are distributed in the area. Figure 4.7 and Figure 4.8 show the initial distribution as well as the resulting

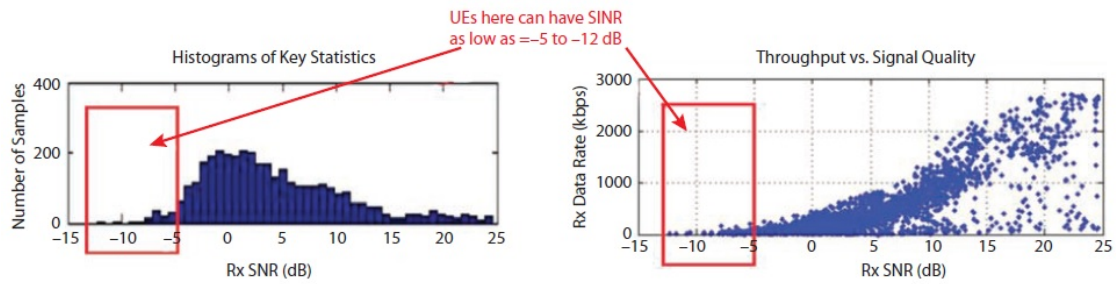


Figure 4.5: The SINR distribution of a real-life OFDMA network with a universal frequency reuse [6].

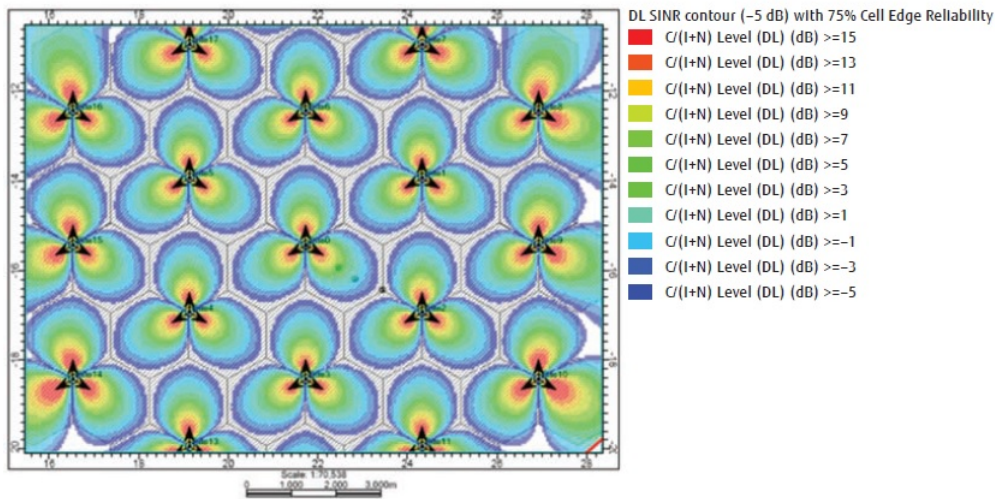


Figure 4.6: Coverage contours of $\text{SINR} = -5$ dB under a universal frequency reuse scenario [6].

planned area for a uniform and a Gaussian distribution of the UEs respectively.

Table 4.2 shows the resulting subset of selected eNodeBs as well as the solving time for the two studied cases. Note that the solving time increases exponentially from 758.96 to 32295.5 with the increase in the number of UEs from 25 to 36. We further extend the problem to account for 40 uniformly distributed UEs, however, after 60,024.5 sec, the lower bound was 2.9916 while the upper bound was 13 and after 161,991.31 sec, the lower bound was 0.999 while the upper bound was 12.99 and no optimal solution was found due to memory limitations. Therefore, we conclude that as the number of variables in the problem increases, the optimal solution for some scenarios becomes difficult to find due to the computational time and the limitation of the memory and hence, the need for a heuristic approach

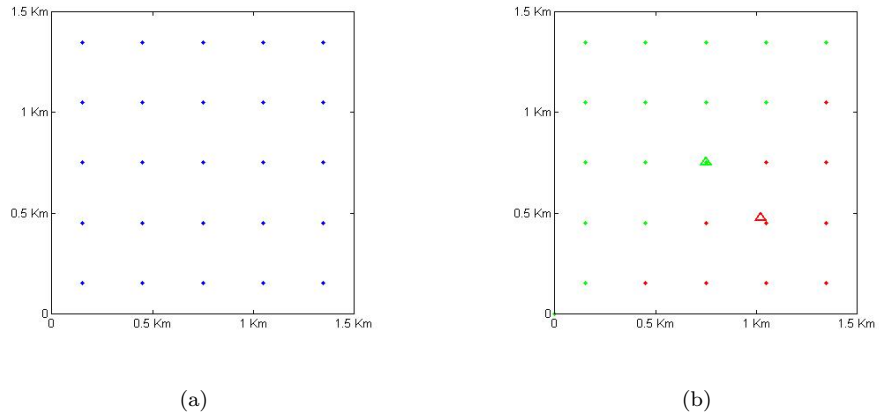


Figure 4.7: (a) The initial distribution and (b) the planned area for a uniform distribution of UEs.

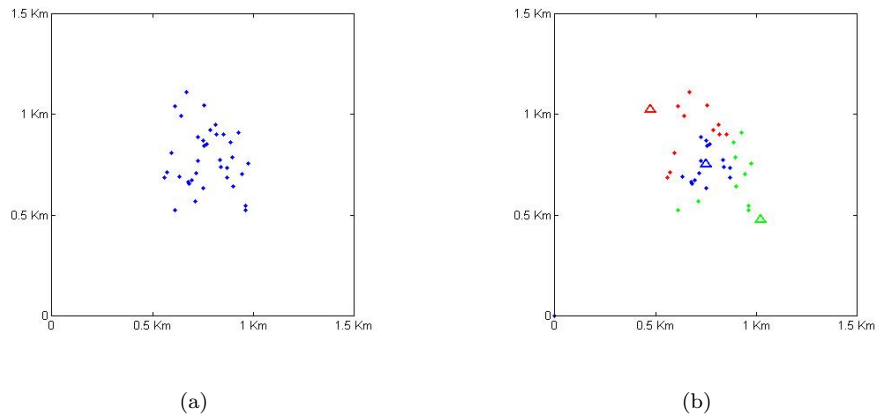


Figure 4.8: (a) The initial distribution and (b) the planned area for a Gaussian distribution of UEs.

rises which will be given later in Section 4.6.

4.5 Site Placement Problem

In this section, we present the site placement problem formulation for LTE RNP under uncertainty. Then, we discuss the complexity of problem.

Table 4.2: The optimal subset of selected eNodeBs and the solving time for the studied cases.

	Selected eNodeBs	Solving time (sec)
case 1	12,13	758.96
case 2	10,12,13	32295.5

4.5.1 Site Placement Problem Formulation

The objective of our problem is to find the optimal location for the deployment of a specific number of eNodeBs in a particular area in order to guarantee that the target threshold SINR for each UE is satisfied with a minimum outage probability. Therefore, we adopt a chance-constraint approach for formulating the optimization problem and we change the stochastic constraints to their corresponding deterministic equivalent. Note that the initial number of eNodeBS can be known from the output of the network dimensioning phase or from some heuristic approach as it will be discussed in Section 4.6. To decide on the eNodeB locations, we define the following decision variables:

$$s_{k,i} = \begin{cases} 1 & \text{if UE } k \text{ is assigned to eNodeB } i, \\ 0 & \text{otherwise} \end{cases}$$

$$a \leq x_i \leq b$$

$$a \leq y_i \leq b$$

Therefore, the site placement optimization problem for LTE RNP under uncertainty is given as follows:

$$\min_{\mathbf{s}, x_i, y_i} \sum_{i=1}^{N_0} \sum_{k=1}^K -s_{i,k} \Pr\{\Gamma_{k,i} \geq \Gamma_{\text{thr}}\} \quad (4.26)$$

subject to

$$e^{\frac{-\sigma^2 \delta_{i,k}^\alpha \Gamma_{\text{thr}}}{\xi_i}} \xi_i \sum_{j=1, j \neq i}^{N_0} \frac{1}{(\xi_i + \delta_{i,k}^\alpha I_{j,k} \Gamma_{\text{thr}}) (\prod_{p=1, p \neq i, p \neq j}^{N_0} (1 - \frac{I_{p,k}}{I_{j,k}}))} \geq (1 - \epsilon) s_{i,k} \quad \forall i, k \quad (4.27)$$

$$\sum_{i=1}^{N_0} s_{i,k} = 1 \quad \forall k \quad (4.28)$$

$$\sum_{k=1}^K s_{i,k} \leq N_c \quad \forall i \quad (4.29)$$

$$s_{i,k} \in \{0, 1\}, a \leq x_i \leq b, a \leq y_i \leq b \quad (4.30)$$

The objective (4.26) maximizes the total probability that the SINR of the UEs k , served by eNodeB i , being greater than a threshold value, i.e. $\Pr\{\Gamma_{k,i} \geq \Gamma_{\text{thr}}\}$. The objective function is non-linear in this case. Note that we have evaluated the site placement problem for different objectives such as proximity and total maximum received power; However, neither proximity nor total max received power are particularly good objectives. Constraint (4.27) represents the quality of service in the network and is derived from the CDF expression of equation (4.12). If $s_{i,k} = 1$, i.e., if UE k is served by eNodeB i , then this guarantees that the probability that $(\Gamma_k \geq \Gamma_{\text{thr}})$ is greater than or equal to $(1-\epsilon)$. If $s_{i,k} = 0$, i.e., if UE k is not served by eNodeB i , then the right hand side is set to zero, and constraint (4.27) is feasible. Note that constraints (4.27) are redundant and non-linear. The non-linearity in the objective function and constraints (4.27) rises from $\delta_{i,k}$ and from the dependance of the interference term I on (x_i, y_i) , the coordinates of the eNodeBs. Constraints (4.28) ensures that every UE in the network is served by exactly one eNodeB in order to maximize the number of served UEs since each eNodeB has a limited capacity. Each eNodeB i can serve at most N_c UEs as shown in constraints (4.29). Finally, constraints (4.30) set the decision variables $s_{i,k}$ to be binary and the decision variables x_i and y_i to be continuous and limited between a and b that represent the dimensions of the area.

4.5.2 Site Placement Problem Complexity

The formulated site placement LTE RNP problem under uncertainty is NP-hard. The problem type is mixed integer non-linear program (MINLP), it involves a nonlinear objective function (4.26) as well as nonlinear inequality constraints (4.27). If we restrict our model to contain only linear functions, MINLP reduces to a mixed integer linear program (MILP), which is an NP-hard problem. On the other hand, if we restrict our model to have no integer variables but allow for general nonlinear functions in the objective or the constraints, then MINLP reduces to NLP which is also known to be NP-hard [50]. Hence, the determination of a global solution to our problem is NP-hard.

One can show that the site placement problem is not tractable, i.e., inefficient to solve. Therefore, in the following section, we develop a heuristic method for solving the site placement optimization formulation.

4.6 Radio Network Planning Algorithm under Uncertainty

For low traffic areas, the site selection problem is solved by Baron within some computational time. However, as the size of the problem increases, the optimal solution for some scenarios becomes difficult to find because of the computational time and the limitation of the memory. Moreover, it has been shown in Section 4.5.2 that the site placement problem formulation is not tractable. Therefore, we develop in this section a site placement algorithm as well as an algorithm for RNP that considers both the site selection problem formulation as well as the site placement algorithm for planning a particular area under uncertainty. Before we give the algorithmic descriptions, we first aim at giving a general background about some important concepts adopted in the algorithms such as K-means clustering, Lloyd's algorithm and steepest descent method.

4.6.1 K-means Clustering

Clustering is the process of grouping a set of objects in such a way that objects in the same group are homogeneous and more similar to each other than to those in other groups based on some measurement criteria. There has been many different approaches for solving the clustering problem such as K-Means, spectral clustering, mean-shift, hierarchical clustering. However, in this section we focus on K-means clustering due to its scalability and efficiency as compared to other methods.

The K-means clustering is a distance-based approach where the objective is to partition a set of data observations into smaller clusters where each observation is set to belong to a particular group such that the resulting assignment minimizes the sum of squares of the distance from the observation point to the mean of the corresponding cluster [51]. The objective formulation is given as follows:

$$\min_{\mathbf{s}} \sum_{i=1}^k \sum_{x_j \in S_i} \|x_j - \mu_i\|^2 \quad (4.31)$$

where S_i represents the i^{th} cluster, x_j represents an observation points, and μ_i represents the mean of the points in cluster S_i . Finding the optimal solution to the k-means clustering problem is known to be NP-hard. Therefore, many efficient heuristic algorithms have been employed that converge quickly to a local optimum. The most common algorithm is the Lloyd's algorithm that uses an iterative technique for solving the optimization problem. The Lloyd's k-means algorithm is described as follows [52]:

1. Choose k points in the space to represent the initial location of the centroids.

2. Assign each observation point to the group that has the closest centroid.
3. Find the new positions of the K centroids by calculating the mean of the observation points in each cluster.
4. Repeat steps 2 and 3 until the centroids do not move significantly.

Although the algorithm does not converge to a global optimal, it has been frequently used due to its ease of implementation. The Lloyd's k-means algorithm has a polynomial smoothed running time in n and $1/\sigma$, where σ is the standard deviation of the Gaussian perturbations [52].

4.6.2 Lloyd's Algorithm

Lloyd's algorithm is also known as Voronoi iteration. Since it is usually hard to jointly optimize clusters and assignment, Lloyd's algorithm is based on optimizing one given the other. Lloyd's method can be found in [53] and is summarized as follows:

1. Select an initial set of k points $c_{i=1}^k$
2. Construct the Voronoi tessellation $V_{i=1}^k$ associated with the points $c_{i=1}^k$.
3. Compute the mass centroids of Voronoi regions $V_{i=1}^k$ found in Step 2; these centroids are the new set of points k and are computed as:

$$z = \frac{\int_{V_i} s \rho(s) ds}{\int_{V_i} \rho(s) ds} \quad (4.32)$$

where ρ is the density function, z is the mass centroid.

4. If this new set of points meets some convergence criterion, terminate; otherwise, return to Step 2

The Lloyd's algorithm is similar to the k-means clustering algorithm in that it repeatedly finds the centroid of each set in the group, and then re-partitions the input according to which of these centroids is closest. However, the difference between both approaches lies in the fact that the input to the Lloyd's algorithm is a continuous geometric region rather than a discrete set of points. Therefore, during the partitioning phase, Lloyd's algorithm uses Voronoi diagrams rather than simply allocating each point to the nearest center as the k-means algorithm does [54].

The computational complexity of the Lloyd's algorithm consists of two phases: the assignment phase and the center update phase. The former requires $O(d \cdot n \cdot K)$ operations, where d is the dimensionality of the data, n the number of data points, and K is the number of centers. The latter is much cheaper and requires $O(d \cdot n)$ operations [55].

4.6.3 Steepest Descent Method

The steepest descent method, also known as the gradient method, is a first-order optimization algorithm. The Taylor representation of the objective function is approximated only with the first two terms in that case. It is a line search method where at every iteration, a search direction p_k and a step size t_k are computed so as to move in the direction that minimizes the objective function. The basic algorithm for any line search method is given in Algorithm 2.

Algorithm 2 Line Search Method

```
while (Not Converged) do  
  choose a search direction,  $p$   
  choose a step size in the search direction,  $t$   
   $x_{k+1} = x_k + t \cdot p$   
   $k = k + 1$   
end while
```

Convergence is met when the gradient is sufficiently small i.e. close to zero. In the first step, a descent direction p that minimizes the objective function is determined. A step size t is determined in the second step. The third step updates the variables to the new value by adding a step size t in the descent direction p . Finally, the fourth step updates the iteration count.

Fixed step sizes will not result in convergence, and exact line searches are generally too expensive; therefore, inexact line searches are used in practice in order to guarantee a sufficient decrease in the objective function and a reasonable progress in the algorithm. The line search method is based on satisfying the Wolfe conditions [56]. The first condition is known as the sufficient decrease condition or the Armijo condition and is given by the following inequality:

$$f(x_k + t \cdot p) \leq f(x_k) + \alpha \cdot \nabla f(x_k)^t \cdot p \cdot t \quad (4.33)$$

To rule out unacceptably short steps, we introduce a second condition known as the curvature condition which requires t to satisfy:

$$\nabla f(x_k + t \cdot p) \geq \gamma \nabla f(x_k)^t \cdot p \quad (4.34)$$

However, the second condition can be neglected if the line search algorithm chooses its candidate step lengths appropriately, by using the backtracking approach where one can start initially with a particular value of t and then backtrack to find a t that satisfies the sufficient decrease condition. For example, one can start initially with a step size that is neither too long nor too short and thus avoids unacceptably short steps and faster convergence. The backtracking line search computes how far one should move along a given search direction. In its most basic form, the backtracking proceeds as given by Algorithm 3 [56].

Algorithm 3 Backtracking Line Search

Choose: $c \in (0, 1)$; $d \in (0, 1)$; and t ;
while $f(x_k + t \cdot p) > f(x_k) + \alpha \cdot \nabla f(x_k)^t \cdot p \cdot t$ **do**
 $t = d \cdot t$;
end while

For the steepest descent direction method, the search direction p is in the opposite direction of the gradient, i.e. $p = -\nabla f(x)$, and therefore, it requires only the computation of the gradient and $O(n)$ storage and work per iteration. It guarantees a global convergence from any starting point, however, with a slow linear rate of convergence, $|f_{k+1} - f^*| < |f_k - f^*|^\alpha$, where the rate of convergence, α , is 1 in that case [56].

4.6.4 Site Placement Algorithm under Uncertainty

Solving the initial site placement optimization problem involves a nonlinear objective function (see (4.26)) and nonlinear inequality constraints (see (4.27)) and thus is an NP-hard problem. Given an initial number and location for the eNodeBs, we aim in this section at developing a heuristic approach for solving the site placement problem. Since it is hard to jointly optimize the location of the eNodeBs and the corresponding assignment, we develop an algorithm that is based on Llyod's algorithm where we aim at optimizing one variable given the other [53]. Therefore, in the proposed algorithm, in one step we fix the assignment variables and solve for the location of the eNodeBs and in the other step we fix the location of the eNodeBs and solve for the optimal assignment variables.

In the first step of the site placement algorithm, we solve for the continuous variables and hence we move the location of the eNodeBs one step in the steepest descent direction of the site placement objective function (4.26). In the second step of the site placement algorithm, we solve for the binary variables and hence we solve the assignment problem and update the $s_{i,k}$ variables. We keep on iterating between both steps until the location of the eNodeBs can not be further moved i.e. when the algorithm converges to optimality. The algorithmic description for the site placement algorithm is given in Algorithm 4. This algorithm achieves a local convergence since the objective function is non-convex.

Note that the optimization problem for the assignment problem is a modification of the site placement problem where we consider fixed locations for the eNodeBs and solve only for the assignment variables. Therefore, the variables in the problem are only $s_{i,k}$. The assignment problem is an ILP problem and can be efficiently solved to optimality using standard ILP solving techniques.

Algorithm 4 Proposed site placement algorithm under uncertainty

Input: $\mathcal{I} = \{i : i = 1, \dots, N_0\}; \mathcal{K} = \{k : 1, \dots, K\}; \{x_i, y_i, i = 1, \dots, N_0\}; \{u_k, v_k, k = 1, \dots, K\}$.

while $\{|x_{i,old} - x_{i,new}| \geq \epsilon \parallel |y_{i,old} - y_{i,new}| \geq \epsilon \parallel (\text{solver status} \neq \text{optimal})\}$ **do**
 Step i. Fix the $s_{i,k}$ variable, move the eNodeBs one step in the steepest descent direction and update the values of x_i and y_i .
 Step ii. Update the values of $s_{i,k}$ by solving the assignment problem with the new values of x_i and y_i .
 if (solver status \neq optimal) **then**
 Retain the old values for the $s_{i,k}$ variables.
 end if
end while

4.6.5 Radio Network Planning Algorithm under Uncertainty

The conventional approach for planning a large network consists of dividing the area of interest into medium/large $d \times d$ areas. The $d \times d$ areas are then classified into 3 types: high traffic, medium traffic, low traffic or no traffic at all. The number of eNodeBs for each region is then estimated through a heuristic approach [57]. Moreover, the uncertainty in the signal's level is neglected, and a deterministic constraint for the QoS is adopted. Therefore, in this section, we develop a new algorithm for dividing the large area into smaller clusters and for finding the optimal location of the eNodeBs taking into account the randomness of the signal and interference levels and thus providing a more realistic approximation for the QoS of the end users. The proposed RNP algorithm combines both the site selection problem formulation and the site placement algorithm in order to find to minimum set of eNodeBs as well as their optimal locations according to the UE's distribution.

For low traffic areas, the site selection problem is solved by Baron within some computational time. However, as the size of the problem increases, the optimal solution for some scenarios becomes difficult to find because of the computational time and the limitation of the memory. Therefore, the proposed radio network planning algorithm under uncertainty consists of initially dividing the area of interest into N clusters, each cluster of r pixels where the set of pixels represent the UEs' distribution in a particular area. To do so, we apply the K-means clustering with an extra equality constraint. If the pixels cannot be divided equally, then the resulting cluster sizes differ in at most one pixel. For each cluster, we solve the site selection optimization problem with an initial distribution of i eNodeBs distributed according to the smallest and largest coordinate of the pixels of the corresponding cluster. The selected subset of eNodeBs for each of the N clusters is denoted as S_n . Then, we merge all the clusters into the original area and lo-

Algorithm 5 Proposed radio network planning algorithm under uncertainty

Input: $\mathcal{K} = \{k : 1, \dots, K\}$; $\{u_k, v_k, k = 1, \dots, K\}$.

Step i. Use K-means clustering with an equality constraint to divide the area of interest into N clusters, each cluster of r pixels.

for $N = N_1 : N_n$ {For each cluster} **do**

Step ii. Solve the site selection problem with i eNodeBs initially distributed according to $u_{k,max}, u_{k,min}, v_{k,max}, v_{k,min}$ of each cluster. Label the subset of selected eNodeBs as S_n .

end for

Step iii. Merge all the clusters into the original area and locate the eNodeBs of the S_n sets, i.e. the selected subset of eNodeBs of each cluster.

Step iv. Consider initially the resulting assignment $s_{i,k}$ variables of the site selection problem for each of the N clusters and solve one iteration of the site placement algorithm.

Step v. Solve the site placement algorithm.

cate the S_n eNodeBs i.e. the selected subset of eNodeBs of each cluster. Now, we apply the site placement algorithm for moving the S_n in order to take into account inter-cluster effect and thus find the optimal location of the eNodeBs. The algorithmic description is given in Algorithm 5.

As the number of variables increases, the solving time of the radio network planning algorithm under uncertainty increases exponentially due to the increase in the size of the gradient and hence its' computation using the finite difference method. Therefore, we adopt a divide and conquer approach for medium and large sized network for faster convergence. The steps followed in this approach are described as follows:

1. Divide the network into D smaller sub-networks where each sub-network is formed by merging P clusters together.
2. Solve the radio network planning algorithm for each of the D sub-networks separately.
3. Merge the D sub-networks into the original network.
4. Run the site placement algorithm for the whole network.

In this approach, we aim at changing the starting point for the site placement algorithm over the large network and thus requiring less iterations to converge to the optimal solution.

4.6.6 Computational Complexity

In the RNP algorithm, the initial site selection solution of each cluster selects the minimal cardinality set of eNodeBs that satisfies the coverage and SINR requirements. This subset serves as an initial starting point for the site placement algorithm, and therefore aims at a faster convergence for the site placement algorithm. In the site placement algorithm, we aim at moving the initial subset of eNodeBs to an optimal location for maximizing the objective function. The cost of solving the assignment problem at every step of the steepest descent is high; however this does not affect the overall running time since the assignment problem is very fast i.e., less than 1 sec. For example, for case study 2, the maximum running time for the assignment problem is 0.3 sec. Therefore, the best running time for the algorithm is the same as that of the steepest descent method i.e., a linear convergence $O(n)$ to the optimal solution. The Broyden-Fletcher-Goldfarb-Shanno (BFGS) search direction can be used instead of the steepest descent direction, with a superlinear convergence rate; however at the cost of $O(n^2)$ storage, and $O(n^2)$ work per iteration. Moreover, at every iteration, the $s_{i,k}$ variables are changing and thus the objective function is changing. However, after some iterations, the $s_{i,k}$ variables do not change anymore and the objective function remains constant and hence the search direction is in the steepest descent direction of this objective function. Figure 4.12 (a) shows a 2-D representation for the contour lines of the objective function with 2 variables. We can note from the contour lines that the objective function is non-convex and hence one cannot claim that the local optimum is the global one. Therefore, we claim that the optimal solution is a local one and thus depends on the initial starting point.

4.7 Results and Analysis of the Radio Network Planning Algorithm under Uncertainty

This section presents results and analysis for the proposed radio network planning algorithm. The proposed site selection formulation is solved using Baron 11 and the assignment problem formulation is solved using Cplex 12.5. We assume that each eNodeB is equipped with an omnidirectional antenna. However, one can apply the developed optimization problems and algorithm to any type or directionality for the antennas. The general simulation parameters used throughout the different scenarios are presented in Table 4.3. Note that the site selection problem is initially solved with an outage percentage, ϵ , of 0.4. This is due to the fact that the site selection problem is solved with a small set of eNodeBs in order to guarantee an optimal solution within some reasonable time due to the complexity of the problem.

Table 4.3: The simulation parameters.

Initial set of eNodeBs i for the site selection problem	9
Max Tx power per eNodeB	42 dBm
Antenna type	Omni-directional
Antenna gain	11 dBi
Cable, connector, and combiner losses	2.5 dB
Noise variance (σ^2)	5.97×10^{-14} W
SINR threshold (Γ_{thr})	-7 dB
Percentage of outage (ϵ)	0.25
Pathloss constant (K)	-80dB
Pathloss exponent (α)	2
Reference distance (d_0)	1

We present in this section four case studies for different density distribution. In order to calculate the steepest descent direction at every iteration of the algorithm, we aim at finding the gradient of the objective function. Therefore, we consider the finite difference approach for the approximation of the gradient. We give a detailed analysis for one small sized network and one medium sized network showing all the steps of the radio network planning algorithm. We show only the initial and the final planned area for the remaining cases to avoid repetition. Note that in all the studied cases, we consider small clusters in order to be able to solve the site selection problem to optimality. This is due to the fact that as the size of the cluster increases, the number of variables in the problem increases and thus finding the optimal solution to the problem becomes difficult due to the limitation on the computational time and memory space.

4.7.1 Small Networks

For small networks, the problem is solved to optimality within a reasonable amount of time. In this section, we provide results and analysis for two case studies of small networks. We give intermediate results for the steps of the radio network algorithm for case study 1 and show only the initial and the final planned area for case study 2.

Case Study 1

We consider in this case study a snapshot 120 UEs uniformly distributed in an area of $1\text{Km} \times 1\text{Km}$ as shown in Figure 4.9. The channel bandwidth is 3 Mhz and the maximum number of UEs that can be served by an eNodeB, N_c , is 15. We divide the area into 4 clusters, each of 30 UEs. The partitioned clusters as well as the initial distribution of the eNodeBs for solving the site selection problem are shown in Figure 4.10. The resulting planned area after solving the site selection problem for each case separately is given in Figure 4.11. Note that the assignment result is not homogeneous because the objective function in that case is not the optimal one to choose. This is further optimized through the assignment problem formulation that is applied in the site placement algorithm.

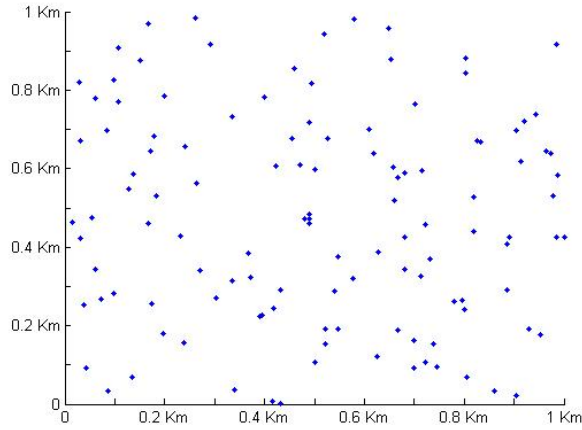


Figure 4.9: The distribution of the UEs for case study 1.

In order to test the effectiveness of the site placement algorithm, we try first to move only one eNodeB (i.e., with only 2 variables, x_i and y_i) in the steepest descent direction with a fixed assignment solution in order to be able to plot the contour lines in a 2-Dimensional space. The contour lines of the objective function and the resulting network after moving the yellow eNodeB are shown in Figures 4.12 (a) and 4.12 (b) respectively. Since our objective function is non-convex, then the resulting optimal solution depends on the starting point of the algorithm. Therefore, according to the initial location of the yellow eNodeB, results validate our algorithm and show that the final position of the yellow eNodeB is at the closest local optimal that minimizes the objective function.

Figure 4.13 (a) shows the objective function value as a function of the iteration number. Moreover, the norm of the gradient as a function of the iteration number

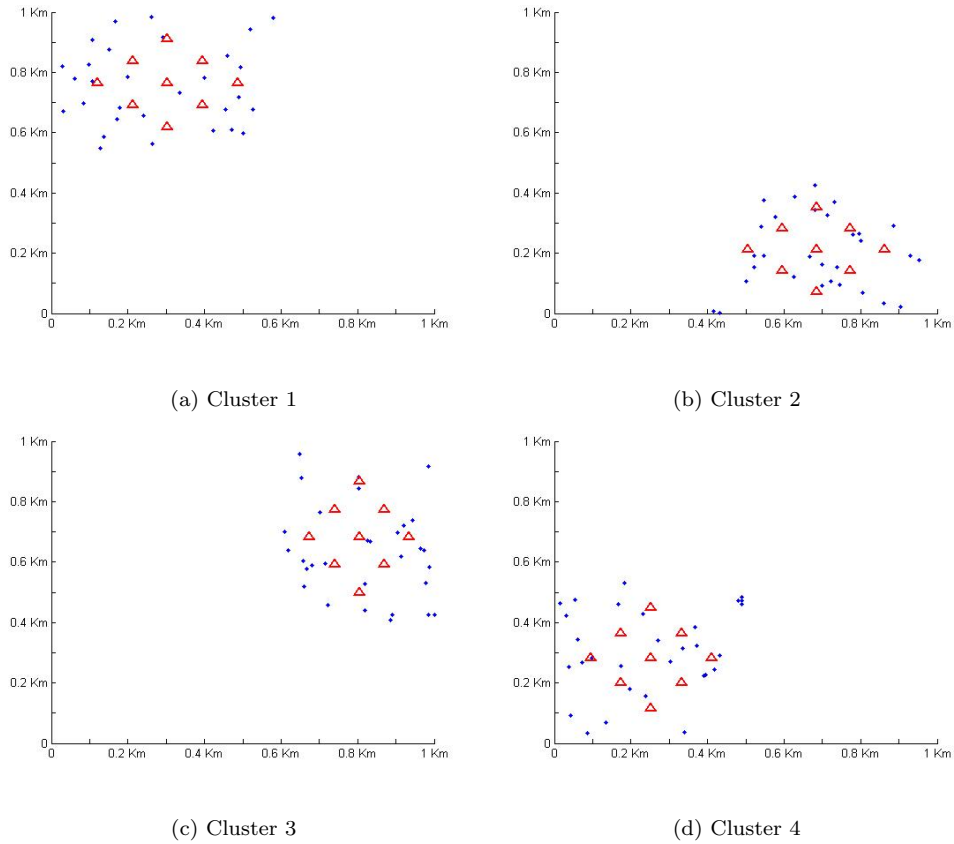


Figure 4.10: The partitioned clusters and initial distribution of the eNodeBs for case study 1.

is shown in Figure 4.13 (b). Figures 4.14 (a) and 4.14 (b) show a semilog plot for the objective function value and norm of the gradient as a function of the iteration number respectively. The linear convergence can be seen from Figure 4.14, especially after the 15th iteration, where the assignment problem, and hence the objective function, remains almost constant afterwards. Results show that after 31 iterations, the value of the objective function remains constant and the norm of the gradient is sufficiently small and thus guarantees optimality. The running time for this scenario is 673 seconds. The output of site placement algorithm, i.e. the final location of the eNodeBs, achieves an increase of approximately 10% in the total outage probability as compared to the initial location of the eNodeBs, i.e. the output of the site selection problem. However, we can notice some peaks in the norm of the gradient during the first few iterations. This is due to the fact that at every iteration the assignment problem is changing and therefore the objective function is changing and thus the steepest descent direction for the

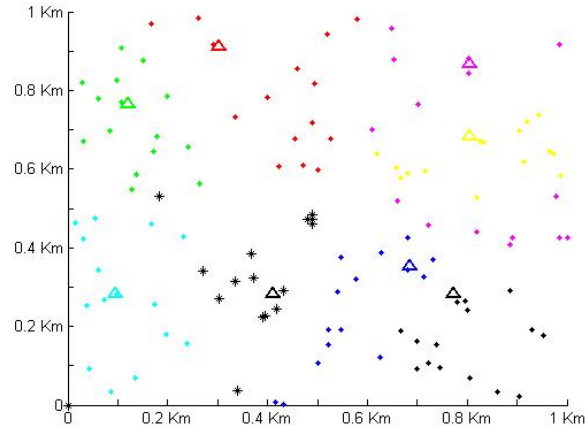


Figure 4.11: The initial planned area for case study 1 after solving the site selection problem.

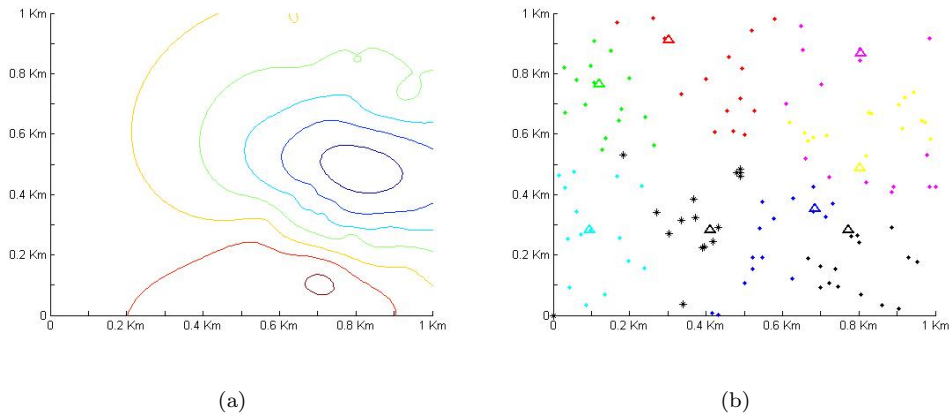


Figure 4.12: (a) The contour lines of the site placement objective function and (b) the resulting planned area after moving the yellow eNodeB in the steepest descent direction of the objective function for case study 1.

new objective function is different. However, after many iterations, the objective slightly changes and at a later stage remains constant and thus the norm of the gradient decreases gradually to zero in the direction of the new objective function. The final planned network as well as the corresponding assignment solution is shown in Figure 4.15.

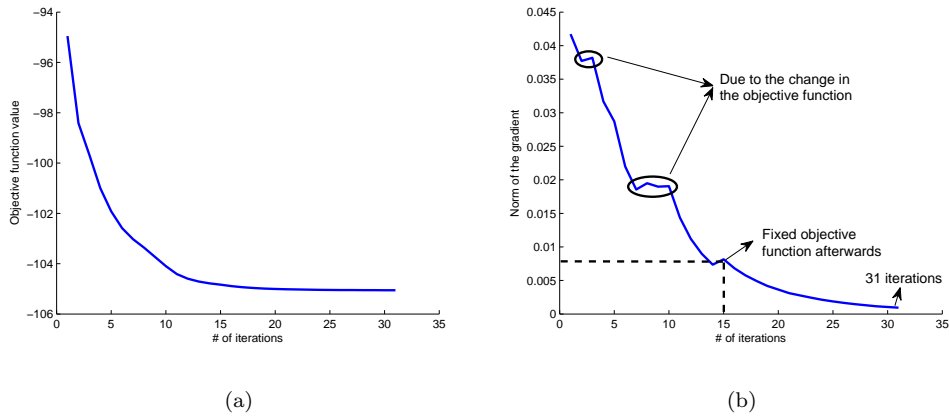


Figure 4.13: (a) The objective function value and (b) the norm of the gradient versus the number of iterations for case study 1.

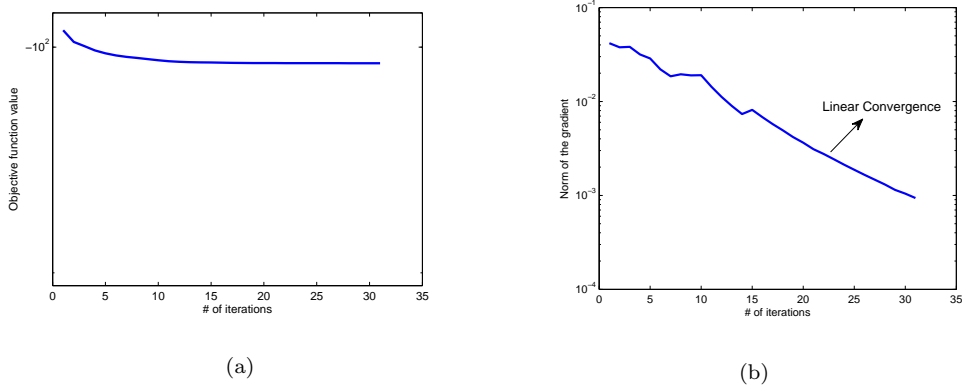


Figure 4.14: A semilog plot for (a) the objective function value and (b) the norm of the gradient versus the number of iterations for case study 1.

Case Study 2

We consider in this case study 198 pixels with a Gaussian distribution at the center of an area of $1\text{Km} \times 1\text{Km}$ as shown in Figure 4.16 (a). The channel bandwidth is 5 Mhz and the maximum number of pixels that can be served by an eNodeB, N_c , is 25. We divide the area into 4 clusters, with 50, 50, 48 and 50 pixels in cluster 1, 2, 3 and 4 respectively. Figure 4.16 (b) shows the resulting planned network for the corresponding pixel distribution. The output of site placement algorithm, i.e. the final location of the eNodeBs, achieves an increase of approximately 40% in the total outage probability as compared to the initial

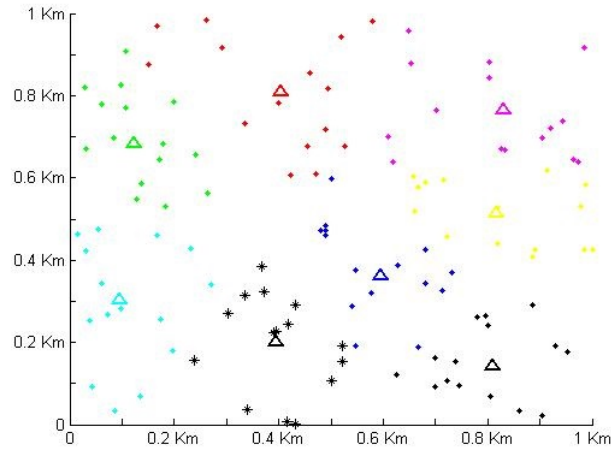


Figure 4.15: The resulting planned network under uncertainty for case study 1 after running the radio network planning algorithm.

location of the eNodeBs, i.e. the output of the site selection problem.

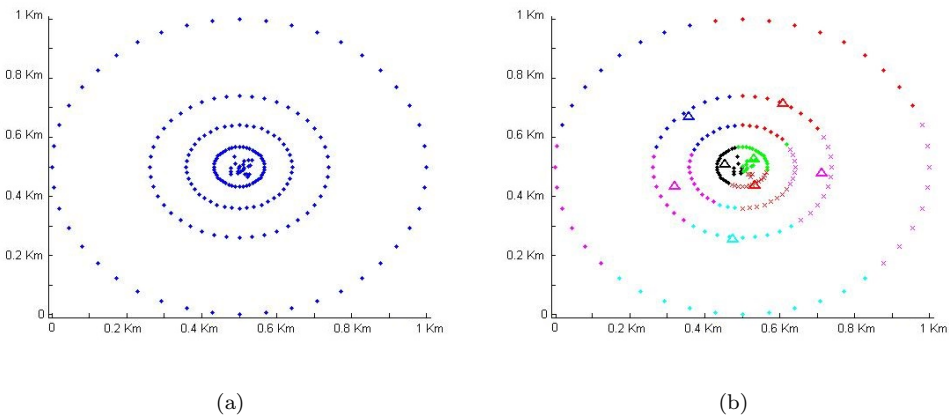


Figure 4.16: (a) The distribution of the pixels and (b) the resulting planned network for case study 2.

4.7.2 Medium to Large Networks

In this section, we provide results and analysis for two case studies of medium sized networks. We give intermediate results for the steps of the radio network

algorithm under uncertainty for case study 3 and show only the initial and the final planned area for case study 4.

Case Study 3

We consider in this case study 400 pixels with 4 Gaussian distributions, each of 100 pixels, at the corners of a 5Km \times 5Km area as shown in Figure 4.17 (a). The channel bandwidth is 5 Mhz and the maximum number of pixels that can be served by an eNodeB, N_c , is 25. We divide the area into 8 clusters, each of 50 pixels. The partitioned clusters as well as the initial distribution of the eNodeBs for solving the site selection problem are shown in Figure 4.18.

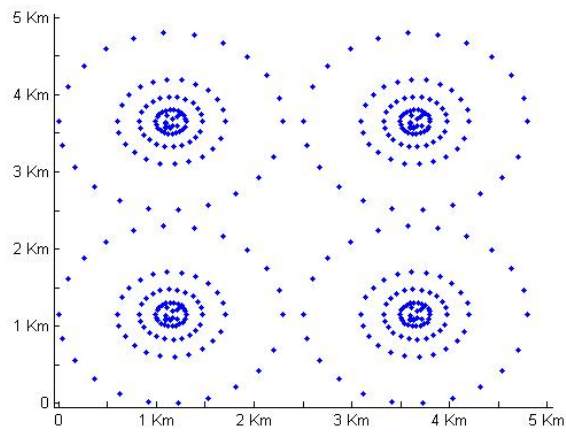
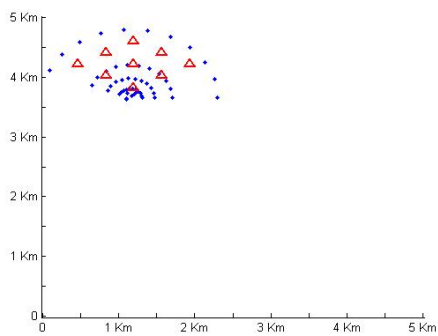
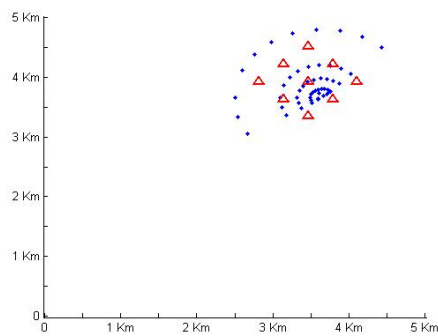


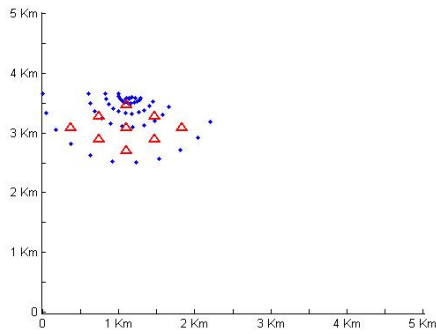
Figure 4.17: The distribution of the pixels for case study 3.



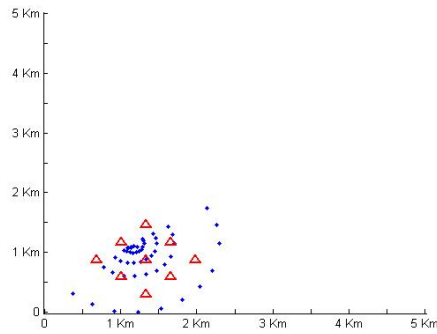
(a) Cluster 1



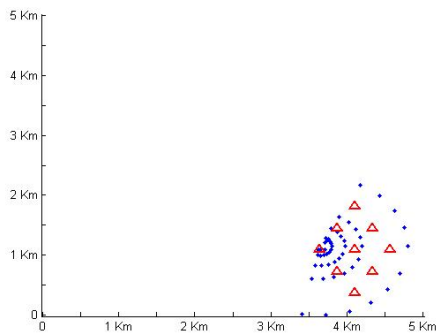
(b) Cluster 2



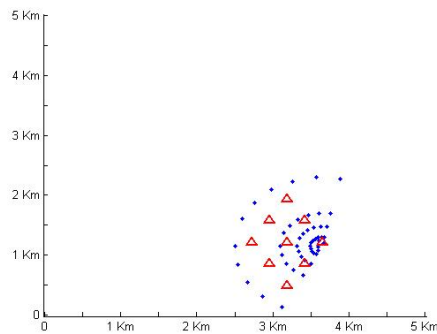
(b) Cluster 3



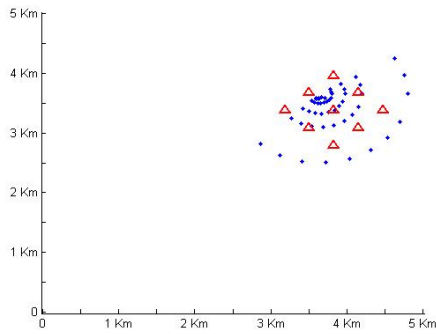
(b) Cluster 4



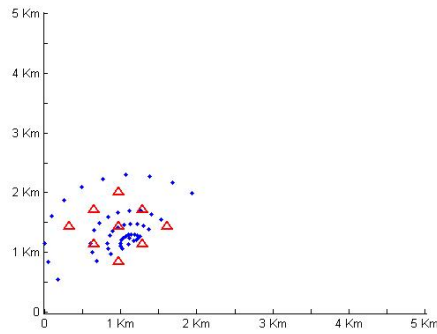
(b) Cluster 5



(b) Cluster 6



(b) Cluster 7



(b) Cluster 8

Figure 4.18: The partitioned clusters and initial distribution of the eNodeBs for case study 3.

We try initially to run the site placement algorithm for all the network; However, after 90 min, the algorithm achieved only 7 iterations with no progress in the planning process and after 3 hours we can note a slight improvement in the planning process and the location of the eNodeBs were still far from the optimal

solution. Therefore, for a faster convergence, we use the divide and conquer approach described earlier since the solving time increases exponentially with the increase in the number of variables due to the computation of the gradient using the finite difference method. We divide the network into 2 large sub-networks, each of 4 clusters, and run the radio network planning algorithm for each separately. The 2 sub-networks are shown in Figure 4.19. The site selection problem result and the site placement algorithm result for sub-networks 1 and 2 are shown in Figures 4.20 and 4.21 respectively. The running time for the site placement algorithm of sub-networks 1 and 2 are 506 and 498 seconds respectively. Then, we merge again the 2 sub-networks, and run the site placement algorithm on the whole network. Figure 4.22 shows the initial and resulting planned network before and after running the site placement algorithm on the merged sub-networks. By adopting this approach, we are changing the initial starting point for the algorithm and thus allowing for a faster convergence since the algorithm would require less number of iterations to converge as compared to the initial distribution of the eNodeBs and the corresponding assignment. In spite of the fact that less number of iterations are required in that case, the running time for 1 iteration increases exponentially with the increase in the size of the network with a slight increase in the QoS on the other hand. Thus, one can neglect the last step in the divide and conquer approach. We can see from Figure 4.22 that there is a slight change in the location of the eNodeBs and the assignment problem for this case study with an increase of less than 1% in the QoS. The final location of the eNodeBs and the corresponding assignment result achieves an increase of approximately 30% in the total outage probability as compared to the initial location of the eNodeBs, i.e. the output of the site selection problem.

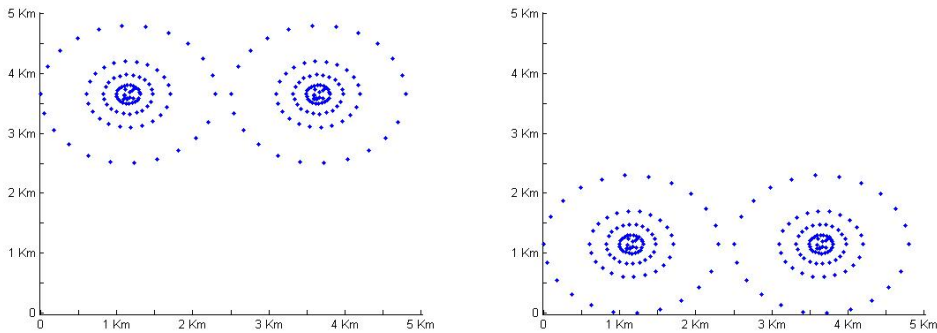


Figure 4.19: The distribution of the pixels for the 2 sub-networks of case study 2.

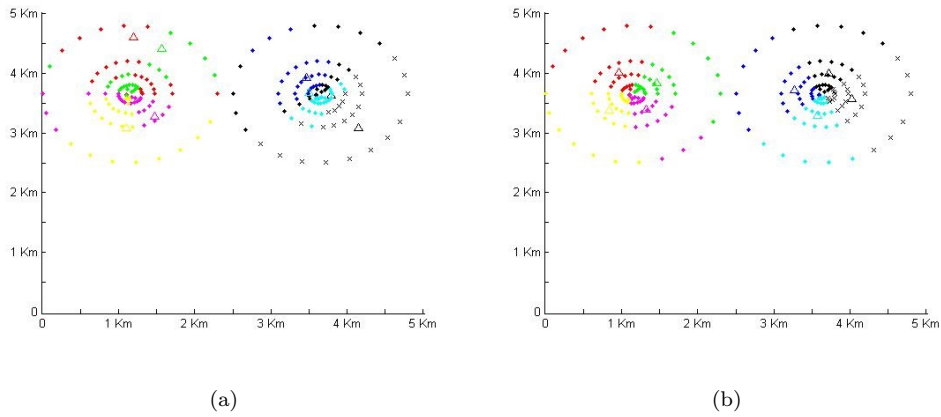


Figure 4.20: (a) The site selection problem result and (b) the site placement algorithm result for subnetwork 1 of case study 3.

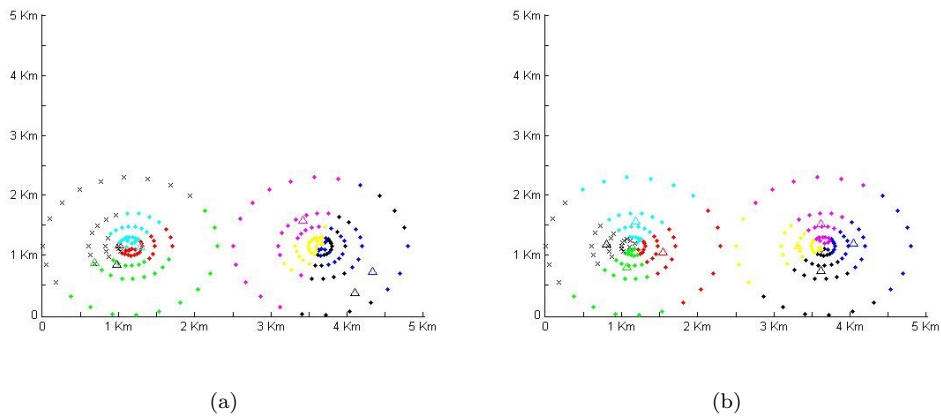


Figure 4.21: (a) The site selection problem result and (b) the site placement algorithm result for subnetwork 2 of case study 3.

Case Study 4

We consider in this case study 550 pixels with a uniform distribution and a hotspot at the center of an area of $5\text{Km} \times 5\text{Km}$ as shown in Figure 4.23 (a). The channel bandwidth is 5 Mhz and the maximum number of pixels that can be served by an eNodeB, N_c , is 25. We divide the area into 11 clusters, each of 50 pixels. Note that as the number of variables increases, the solving time increases. Therefore for a faster convergence, we use a divide and conquer approach described earlier where we divide our network into 3 large sub-networks, two of 4

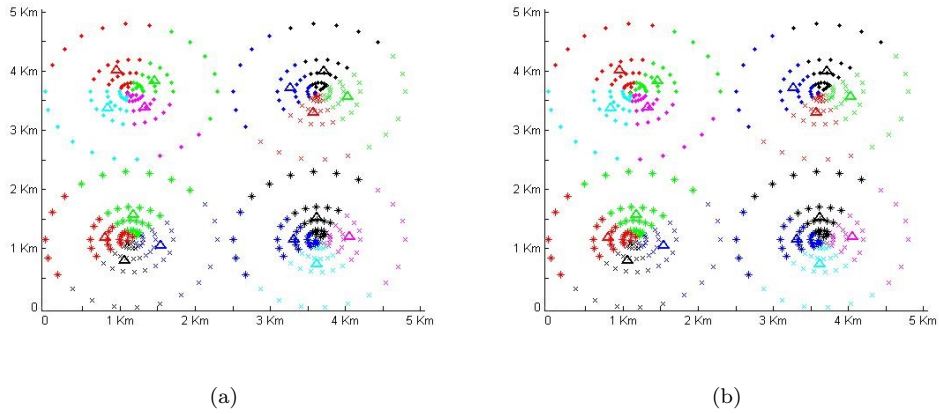


Figure 4.22: (a) The initial and (b) resulting planned network before and after running the site placement algorithm on the merged sub-networks for case study 3.

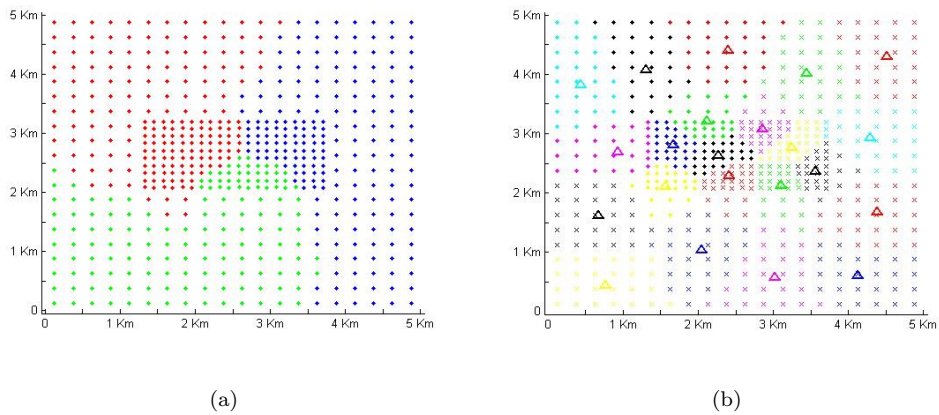


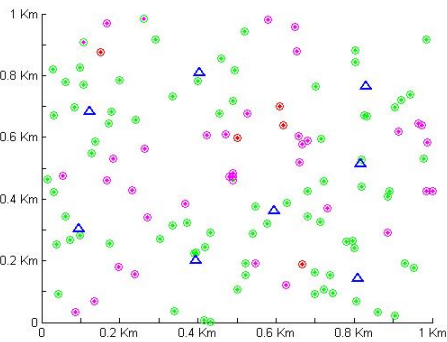
Figure 4.23: (a) The distribution of the pixels as well as the partitioned sub-networks (the three colors of the pixels correspond to the three partitioned sub-networks) and (b) the final planned area after solving the proposed radio network planning algorithm for the whole network of case study 4.

clusters and one of 3 clusters, and run the radio network planning algorithm for each separately. Then, we merge again these 3 large sub-networks, and run the site placement algorithm on the whole network. By adopting this approach, we are changing the initial starting point for the algorithm and thus allowing for a faster convergence. Figure 4.23 (b) shows the resulting planned network for the corresponding pixel distribution. The final location of the eNodeBs and the cor-

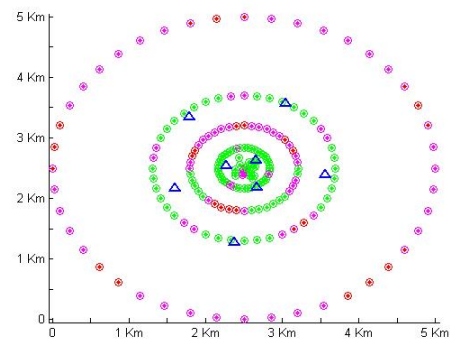
responding assignment result achieves an increase of approximately 25% in the total outage probability as compared to the output of the site selection problem.

4.7.3 Monte Carlo Simulation Results

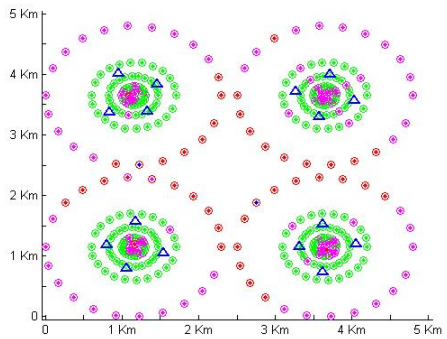
Because of the trade-off between coverage, capacity, and service quality in an LTE network, network planning applications require an accurate simulator to provide detailed and statistically relevant information on expected network performance. Therefore, we run monte carlo simulations for the resulting planned networks taking into account the uncertainty in the signals' level due to Rayleigh fading and we compare it to the results of the proposed chance-constraint approach. The results for both approaches for the studied cases are given in Figure 4.24. It can be seen from Figure 4.24 that the monte carlo simulations and the chance-constraint approach result in the same probability of $(\Gamma_k \geq \Gamma_{thr})$ and therefore validate our simulation results.



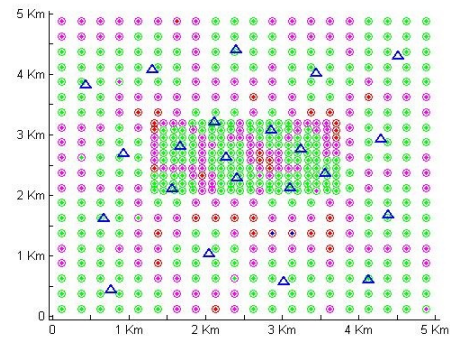
(a) Case study 1



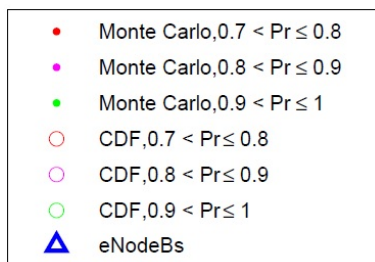
(b) Case study 2



(c) Case study 3



(d) Case study 4



(e) Legend

Figure 4.24: The monte carlo simulation results for the studied cases.

4.8 Summary

In conventional RNP, the uncertainty in the signal and interference levels is not taken into account during the planning process. Operators consider the channel of the UEs to be deterministic and plan a network according to a given outage parameter. In this chapter, we have presented a two-stage chance constraint approach for planning an LTE network under signal and interference level uncertainty. Moreover, we have developed an algorithm for determining the optimal location of the eNodeBs.

The typical operator's aim is to optimize the network according to coverage and capacity. Call drop rates give a first indication for areas with insufficient coverage, traffic counters identify capacity problems. Therefore, the use of the chance constraint approach, as illustrated in this chapter, allows the following objectives to be achieved as compared to the traditional approach:

- Providing better coverage in the network area. This objective requires that in the area, where LTE system is offered, users can establish and maintain connections with acceptable or default service quality, according to operators requirements. In the proposed approach, the capacity of an eNodeB is fixed and the planning is done for coverage. It implies therefore that the coverage is continuous and users are unaware of cell borders and changes according to the traffic state.
- Providing a more realistic and accurate model of the network and thus leading to a more dynamic network that has a better performance.
- Providing better QoS for the end users by taking into account the fading uncertainty. The developed approach considers a probabilistic outage constraint as compared to the conventional approach where a deterministic one is adopted.

- Developing a RNP algorithm to find the optimal location of the eNodeBs and therefore increasing the probability of the UEs for meeting the QoS requirements.

Chapter 5

Conclusions

In this work, we have addressed the problem of LTE radio network planning under system and channel uncertainty. The main objective was to jointly optimize the eNodeB locations and UE assignment to the best server under uncertainty. We have considered two planning approaches; the first under demand uncertainty and the second under signal and interference level uncertainty. In the first part of the thesis work, we have considered a two-stage stochastic approach for LTE RNP under demand uncertainty where our objective is to minimize the number of eNodeBs over a given area and maximize the users' throughput. Traffic demands vary during the day depending on the users' behavior and their data needs and hence, the proposed approach takes into account different traffic distributions at different times of the day and selects the optimal locations for the eNodeBs from a predefined set of candidate locations. Moreover, a dynamic switching on/off eNodeB algorithm is applied to the planned area in order to have an energy efficient network operation. Performance results have shown an increase in the users' throughput when considering uncertainty in the demand as part of the RNP process compared to conventional RNP. It is also shown that the gain of the proposed approach depends on the probability of the traffic states. Moreover, notable energy savings can be obtained upon switching off selected eNodeBs at off-peak hours. In the second part of the thesis work, we have considered a two-stage chance constraint approach for LTE RNP under the uncertainty of the signal and interference levels. The proposed approach takes into account a semi-analytical statistical model for downlink ICI as a function of generic fading models. A site selection problem is formulated and solved for small sized networks. Moreover, a site placement problem is formulated and shown to be NP-hard, and hence an algorithm was proposed to solve the corresponding problem. Finally, we provide a general optimization framework for LTE RNP by developing a radio network planning algorithm under uncertainty that combines the two optimization problems of site selection and site placement in order to find the minimum set of eNodeBs as well as their optimal locations. Monte carlo simulation results validate our algorithm results and hence the proposed planning

approach ensures a reliable network planning under uncertainty.

This work can be extended in many directions:

1. The computation of the gradient increases exponentially with the increase in the number of variables using the finite difference method. Therefore, one future direction for this research work is to investigate faster convergence methods for the computation of the gradient, for instance, automatic differentiation (AD).
2. Take into account the users mobility and thus make the problem more robust. Consider a statistical model for the UEs mobility and develop a stochastic formulation where the expected recourse function is calculated using the mobility statistical model.
3. Take into account other uncertain parameters present in the network, for example, power requirements. Use power control techniques to further decrease power consumption for each traffic state. The power of the eNodeBs may be tuned to reduce power consumption in the network.
4. Consider the machine-to-machine (M2M) radio network planning problem. The first formulation can be easily extended to take into account other types of machines present in the network.
5. The developed formulations and algorithms can be used in practice for actual planning and hence can be implemented in an LTE RNP tool.

Appendix A

Abbreviations

3GPP	Third Generation Partnership Project
AD	Automatic Differentiation
AWGN	Additive White Gaussian Noise
Baron	Branch-And-Reduce Optimization Navigator
BB	Branch and Bound
BFGS	Broyden-Fletcher-Goldfarb-Shanno
BS	Base Station
CCP	Chance-Constraint Programming
CDF	Cumulative Distribution Function
CDMA	Code Division Multiple Access
CFLP	Capacitated Facility Location Problem
DL	Downlink
ECP	Extended Cutting Plane
eNodeB	Evolved NodeB
E-UTRAN	Evolved Universal Terrestrial Access Network
FDD	Frequency Division Duplexing
GBD	Generalized Benders Decomposition
GO	Global Optimization
GSM	Global System for Mobile Communications
HARQ	Hybrid Automatic Repeat Request
HSPA	High Speed Packet Access
ICI	Intercell Interference
ICT	Information and Communication Technology
ILP	Integer Linear Programming
LBA	Link Budget Analysis
LP	Linear Programming
LTE	Long Term Evolution
M2M	Machine-to-Machine
MAPL	Maximum Allowed Path Loss
MGF	Moment Generating Function

MIMO	Multiple Input Multiple Output
MINLP	Mixed Integer Non-Linear Program
MISO	Multiple Input Single Output
MME	Mobility Management Entity
NIP	Nonlinear Integer Program
NLP	Nonlinear Program
OA	Outer Approximation
OFDM	Orthogonal Frequency Division Multiplexing
OFDMA	Orthogonal Frequency Division Multiple Access
OPEX	Operational Expenditure
PDF	Probability Distribution Function
PDN	Packet Data Network
P-GW	Packet Data Network Gateway
QoS	Quality of Service
RB	Resource Block
RF	Radio Frequency
RNP	Radio Network Planning
RNPO	Radio Network Planning and Optimization
RO	Robust Optimization
RV	Random Variable
SC-FDMA	Single Carrier Frequency Division Multiplexing
SCFLP	Stochastic Capacitated Facility Location Problem
S-GW	Serving Gateway
SINR	Signal to Interference and Noise Ratio
SP	Stochastic Programming
SUFLP	Stochastic Uncapacitated Facility Location Problem
TDD	Time Division Duplexing
TS	Tabu Search
UE	User Equipment
UL	Uplink
UMTS	Universal Mobile Telecommunications System

Bibliography

- [1] 3GPP TS 36.300, “Evolved Universal Terrestrial Radio Access (E-UTRA) and Evolved Universal Terrestrial Radio Access Network (E-UTRAN),” tech. rep., 2008.
- [2] D. Talbot, “Glimpses of a world revealed by cell-phone data.” <http://www.technologyreview.com/news/514646/glimpses-of-a-world-revealed-by-cell-phone-data/>, May 2013.
- [3] NationMaster.com, “Rayleigh fading.” <http://www.statemaster.com/encyclopedia/Rayleigh-fading>, December 2013.
- [4] P. Bernardin, M. F. Yee, and T. Ellis, “Cell radius inaccuracy: a new measure of coverage reliability,” *IEEE Transactions on Vehicular Technology*, vol. 47, no. 4, pp. 1215–1226, November 1998.
- [5] H. Yang, “Simple formulas for area coverage probability of cellular wireless networks,” *5th IEEE Vehicular Technology Conference (VTC Spring 2012)*, May 2012.
- [6] FujitsuWhitePaper, “Enhancing LTE cell-edge performance via PDCCH ICIC,” 2011.
- [7] T. L. Magnanti, P. Mirchandani, and R. Vachani, “Modelling and solving the two-facility capacitated network loading problem,” *Operational Research*, vol. 43, no. 1, pp. 142–157, February 1995.
- [8] A. A. Khalek, L. Al-Kanj, Z. Dawy, and G. Turkiyyah, “Optimization models and algorithms for joint uplink/downlink UMTS radio network planning with SIR-based power control,” *IEEE Transactions on Vehicular Technology*, vol. 60, no. 4, pp. 1612–1625, May 2011.
- [9] W. El-Beaino, A. M. El-Hajj, and Z. Dawy, “A proactive approach for lte radio network planning with green considerations,” *19th International Conference on Telecommunications (ICT 2012)*, April 2012.

- [10] E. Amaldi, A. Capone, and F. Malucelli, "Radio planning and coverage optimization of 3G cellular networks," *Wireless Networks*, vol. 14, no. 4, pp. 435–447, August 2008.
- [11] L. Al-Kanj, Z. Dawy, and G. Turkiyyah, "A mathematical optimization approach for cellular radio network planning with co-siting," *Wireless Networks*, vol. 18, no. 5, pp. 507–521, June 2012.
- [12] J. R. Birge and F. Louveaux, *Introduction to Stochastic Programming*. Springer, 1997.
- [13] L. V. Snyder, "Facility location under uncertainty: a review," *IIE Transactions*, vol. 38, no. 7, pp. 537–554, May 2006.
- [14] K. Iwamura and B. Liu, "A genetic algorithm for chance constrained programming," *Information & Optimization Sciences*, vol. 17, no. 2, pp. 409–422, 1996.
- [15] J. Ren, R. Zhao, and B. Liu, "The combination model of stochastic optimal depenture investment," *The Theory and Practice of Systemic Engineering*, vol. 9, no. 1, pp. 14–18, 2000.
- [16] S. He, S. S. Chaudhry, Z. Lei, and W. Baohua, "Stochastic vendor selection problem: chance constrained model and genetic algorithms," *Annals of Operations Research*, vol. 168, no. 1, pp. 169–179, April 2009.
- [17] A. Soyster, "Convex programming with set-inclusive constraints and applications to inexact linear programming," *Operations Research*, vol. 21, no. 5, pp. 1154–1157, October 1973.
- [18] A. Ben-Tal and A. Nemirovski, "Robust solutions of linear programming problems contaminated with uncertain data," *Mathematical Programming*, vol. 88, no. 3, pp. 411–424, June 2000.
- [19] D. Bertsimas and M. Sim, "The price of robustness," *Operations Research*, vol. 52, no. 1, pp. 35–53, February 2004.
- [20] E. Amaldi, A. Capone, and F. Malucelli, "Improved models and algorithms for UMTS radio planning," in *Proceedings of the IEEE Vehicular Technology Conference*, pp. 920–924, October 2011.
- [21] E. Amaldi, A. Capone, and F. Malucelli, "Optimizing base station siting in UMTS networks," in *Proceedings of the IEEE Vehicular Technology Conference*, pp. 2828–2832, October 2001.

- [22] E. Amaldi, A. Capone, F. Malucelli, and F. Signori, "Optimization models and algorithms for downlink UMTS radio planning," in *Proceedings of IEEE WCNC*, pp. 827–831, March 2003.
- [23] E. Amaldi, A. Capone, and F. Malucelli, "Planning UMTS base station location: optimization models with power control and algorithms," *IEEE Transactions on Wireless Communication*, vol. 2, no. 5, pp. 939–952, September 2003.
- [24] S. Hurley, "Planning effective cellular mobile radio networks," *IEEE Transactions on Vehicular Technology*, vol. 51, no. 2, pp. 243–253, March 2002.
- [25] H. Sherali, C. Pendyala, and T. Rappaport, "Optimal location of transmitters for micro-cellular radio communication system design," *IEEE Journal on Selected Areas in Communications*, vol. 14, no. 4, pp. 662–673, May 1996.
- [26] W. El-Beaino, A. M. El-Hajj, and Z. Dawy, "A proactive approach for LTE radio network planning with green considerations," *19th International Conference on Telecommunications (ICT)*, April 2012.
- [27] S. Boiardi, A. Capone, and B. Sanso, "Radio planning of energy-efficient cellular networks," *21st International Conference on Computer Communications and Networks (ICCCN)*, July 2012.
- [28] J. M. Rosenberger and E. V. Olinick, "Robust tower location for code division multiple access networks," *Naval Research Logistics*, vol. 54, no. 2, pp. 151–161, March 2007.
- [29] A. Eisenblatter and J. Schweiger, "Multistage stochastic programming in strategic telecommunication network planning," *Computational Management Science*, vol. 9, no. 3, pp. 303–321, September 2011.
- [30] P. Brevis, J. Gondzio, Y. Fan, H. Poor, J. Thompson, and I. Krikidis, "Base station location optimization for minimal energy consumption in wireless networks," *73rd Vehicular Technology Conference (VTC 2011)*, May 2011.
- [31] G. Claen, A. Koster, and A. Schmeink, "Robust planning of green wireless networks," *5th International conference on Network Games, Control and Optimization (NetGCOOP 2011)*, October 2011.
- [32] A. Koster, M. Kutschka, and C. Raack, "Cutset inequalities for robust network design," in *Proceedings of the International Network Optimization Conference (INOC 2011)*, vol. 6701 of *Lecture Notes on Computer Science*, pp. 118–123, 2011.

- [33] A. Koster, M. Kutschka, and C. Raack, “Robust network design: formulations, valid inequalities, and computations,” *Networks*, vol. 61, no. 2, pp. 128–149, March 2013.
- [34] A. Ouorou and J.-P. Vial, “A model for robust capacity planning for telecommunications networks under demand uncertainty,” *6th International Workshop on Design and Reliable Communication Networks (DRCN 2007)*, October 2007.
- [35] H. W. Lee and S. Chong, “Downlink resource allocation in multicarrier systems: frequency-selective vs. equal power allocation,” *IEEE Transactions on Wireless Communications*, vol. 7, no. 10, pp. 3738–3747, October 2008.
- [36] 3GPP TR 25.942 v2.1.3, “3rd Generation Partnership Project; Technical Specification Group (TSG) RAN WG4; RF System Scenarios,” tech. rep., 2000.
- [37] J. Laiho, A. Wacker, and T. Novosad, eds., *Radio Network Planning and Optimisation for UMTS*. Wiley, 2 ed., February 2006.
- [38] L. V. Snyder, “Facility location under uncertainty: a review,” *IIE Transactions*, vol. 38, no. 7, pp. 547–564, May 2006.
- [39] R. Ravi and A. Sinha, “Hedging uncertainty: approximation algorithms for stochastic optimization programs,” *Mathematical Programming*, vol. 108, no. 1, pp. 97–114, August 2006.
- [40] IBM, *IBM ILOG AMPL user’s guide*, 12.1 ed., June 2009.
- [41] J. Malmodin, A. Moberg, D. Lunden, G. Finnveden, and N. Lovehagen, “Greenhouse gas emissions and operational electricity use in the ICT and entertainment & media sectors,” *Industrial Ecology*, vol. 14, no. 5, pp. 770–790, October 2010.
- [42] A. Fehske, G. Fettweis, J. Malmodin, and G. Biczok, “The global footprint of mobile communications: the ecological and economic perspective,” *IEEE Communication Magazine*, vol. 49, no. 8, pp. 55–62, August 2011.
- [43] Z. Hasan, H. Boostanimehr, and V. Bhargava, “Green cellular networks a survey, some research issues and challenges,” *IEEE Communications Surveys & Tutorials*, vol. 13, no. 4, pp. 524–540, September 2011.
- [44] A. Chatzipapas, S. Alouf, and V. Mancuso, “On the minimization of power consumption in base stations using on/off power amplifiers,” *IEEE Online Conference on Green Communications (GreenCom 2011)*, September 2011.

- [45] N. Akl, J. Fahs, and Z. Dawy, “Statistical intercell interference modeling for capacity coverage tradeoff analysis in downlink cellular networks,” tech. rep., American University of Beirut.
- [46] J. Hmlinen, “Cellular network planning and optimization part ii: fading,” tech. rep., Helsinki University of Technology, January 2007.
- [47] D. Reudink, *Microwave Mobile Communications*, ch. 2, pp. 126–128. *IEEE Press*, 1996.
- [48] W. Xu, X. Wang, and S. Alshomrani, “Probability-constrained power optimization for multiuser MISO systems with imperfect CSI: a bernstein approximation approach,” *CoRR*, vol. abs/1303.4567, 2013.
- [49] N. Soltani, S. Kim, and G. B. Giannakis, “Chance-constrained optimization of OFDMA cognitive radio uplinks,” *IEEE Transactions on Wireless Communications*, vol. 12, no. 3, pp. 1098–1107, March 2013.
- [50] S. Burer and A. N. Letchfordb, “Non-convex mixed-integer nonlinear programming: a survey,” *Surveys in Operational Research and Management Science*, vol. 97, no. 106, pp. 97–106, August 2012.
- [51] D. Arthur, B. Manthey, and H. Roglin, “Smoothed analysis of the k-means method,” *Journal of the ACM (JACM)*, vol. 58, no. 19, October 2011.
- [52] D. Arthur, B. Manthey, and H. Röglin, “K-means has polynomial smoothed complexity,” *CoRR*, vol. abs/0904.1113, 2009.
- [53] Q. Du, V. Faber, and M. Gunzburger, “Centroidal voronoi tessellations: applications and algorithms,” *SIAM Review*, vol. 41, no. 4, pp. 637–676, March 1999.
- [54] M. Emelianenko, L. Ju, and A. Rand, “Nondegeneracy and weak global convergence of the Lloyd algorithm in R^D ,” *SIAM Journal on Numerical Analysis*, vol. 46, no. 3, pp. 1423–1441, March 2008.
- [55] P. Eliasson and N. Rosen, “Efficient k-means clustering and the importance of seeding,” Master’s thesis, KTH Computer Science and Communication.
- [56] J. Nocedal and S. J. Wright, *Numerical Optimization*. Springer, 2nd ed., 2006.
- [57] E. Amaldi, A. Capone, F. Malucelli, and F. Signori, “UMTS radio planning: optimizing base station configuration,” in *Proceedings of IEEE Vehicular Technology Conference*, pp. 768–772, September 2002.